GEOSCIENCE AUSTRALIA

Australian Government

Geoscience Australia

Potential for magmatic-related uranium mineral systems in Australia

Anthony Schofield

Record

2010/20

GeoCat # 70389

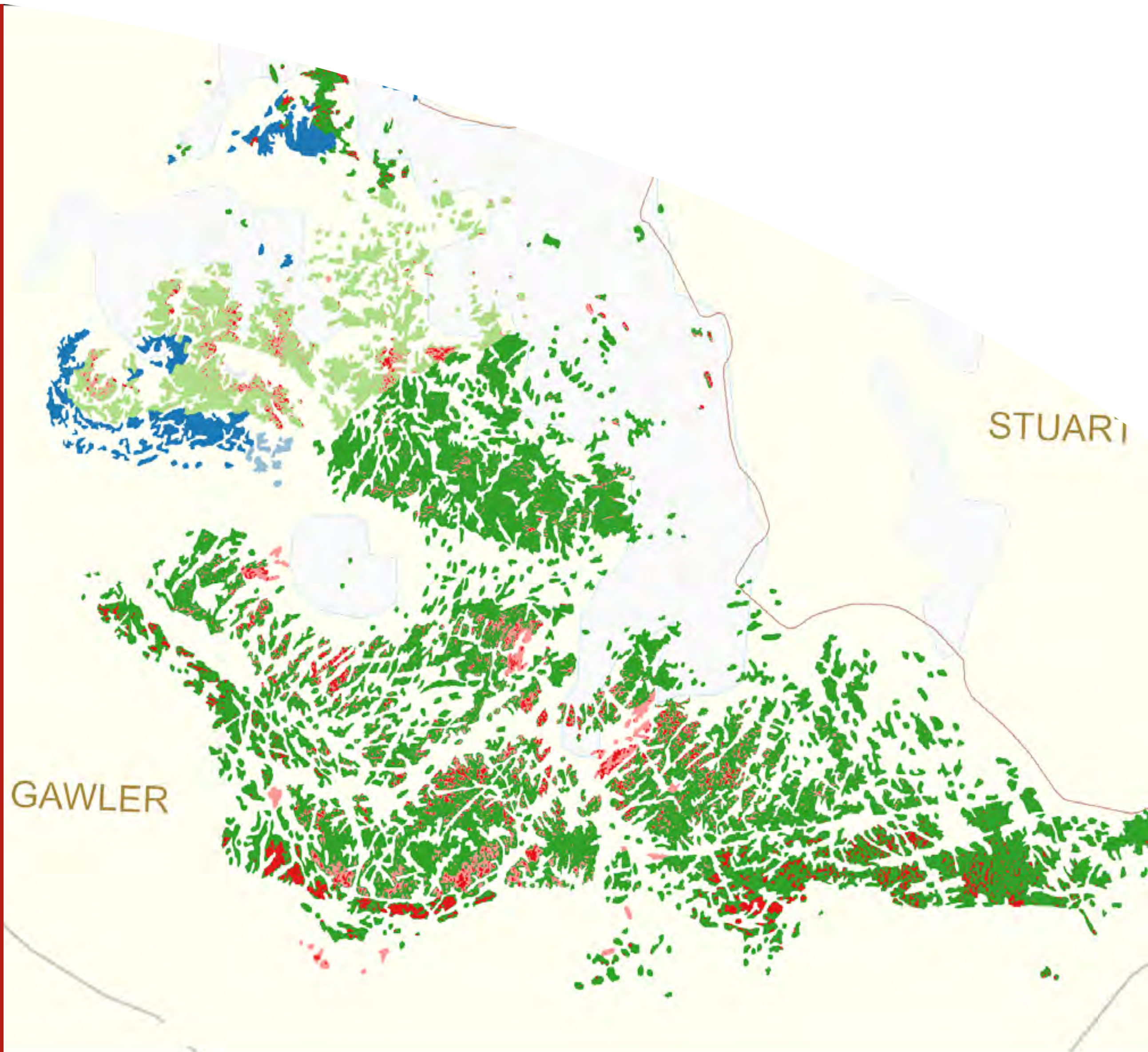

APPLYING GEOSCIENCE TO AUSTRALIA'S MOST IMPORTANT CHALLENGES

Potential for magmatic-related uranium mineral systems in Australia

GEOSCIENCE AUSTRALIA
RECORD 2010/20

by

Anthony Schofield

1. Onshore Energy and Minerals Division, Geoscience Australia, GPO Box 378, Canberra, ACT 2601

Department of Resources, Energy and Tourism
Minister for Resources and Energy: The Hon. Martin Ferguson, AM MP
Secretary: Mr Drew Clarke

Geoscience Australia
Chief Executive Officer: Dr Chris Pigram

ISSN 1448-2177
ISBN 978-1-921781-06-3 print
ISBN 978-1-921781-04-9 web

GeoCat # 70389

Bibliographic reference: Schofield, A., 2010. Potential for magmatic-related uranium mineral systems in Australia. Geoscience Australia Record, 2010/20, 56p.

Contents

Executive Summary

Australia's currently known magmatic-related uranium resources are low, despite the widespread occurrence of uranium-rich igneous rocks nationwide. This discrepancy suggests that Australia is under-represented in this family of uranium mineral systems, and therefore there is high potential for new discoveries of magmatic-related mineralisation. An assessment of the potential for magmatic-related uranium systems has been made using the fuzzy logic method. This method has been selected due to its flexibility, ease of use, and ability to account for uncertainty.

Two subcategories of magmatic-related uranium systems have been assessed for: intrusive- and volcanic-related. Mappable prospectivity criteria have been developed for each of these subcategories based on a mineral systems approach. In many cases, the criteria are identical for both systems, since both are underpinned by the same fundamental processes of partial melting, uranium solubility and fractional crystallisation. Other criteria are specific to the targeted subcategory.

The investigation has not attempted to identify specific sites of uranium mineralisation, but has rather focused on identifying igneous events and units which exhibit favourability for magmatic-related uranium systems. Potentially prospective units for each subcategory occur in all States and Territories. In many cases, identified prospective units occur in regions where uranium potential has been proven, including the Pine Creek, Curnamona and Georgetown-Cairns regions. Furthermore, potential has also been identified in regions not currently known for uranium mineralisation, including the Arunta, Musgrave and Halls Creek regions. The results of this study provide an initial tool for targeting magmatic-related uranium systems. This broad assessment should be further refined on a regional scale, making use of detailed local datasets and knowledge.

Introduction

Recent work by Skirrow et al. (2009) has identified three end-member ‘families’ of U mineral systems, with a number of ‘hybrid’ styles in between. Magmatic (and magmatic-hydrothermal) U systems form one such end-member. Genetically, this family of U system is primarily associated with igneous processes, including partial melting, magmatic evolution, and the influence of magmatic fluids. This differentiates magmatic-related U systems from other ‘hybrid’-type systems, which may also have a genetic association with igneous rocks, such as IOCG-U. Mineralisation associated with igneous rocks constitutes only a small proportion of Australia’s total known resources of U (McKay and Miezitis, 2001), despite the widespread occurrence of U-enriched igneous rocks across the continent (Lambert et al., 2005; Schofield, 2009). Known intrusive-related mineralisation is almost entirely restricted to South Australia, while volcanic-related mineralisation is known mostly from northern Queensland.

The lack of major magmatic-related U deposits in Australia presents a significant opportunity for new discoveries. GIS-based analysis offers a powerful tool for assessing the prospectivity for U mineral systems at the regional to continental scale. Prospectivity modelling has recently been applied to a number of different U-related systems, including IOCG (Nykänen et al., 2008) and hydrothermal breccia/skarn/vein (Cowley et al., 2009). Recently, prospectivity analysis methodologies have been applied to northern Queensland for a range of U systems, including those associated with magmatism (Huston, 2010). Other qualitative assessments have been undertaken elsewhere, and have focused on identifying analogous tectonic and geological features to known deposits (for example, Rogers et al., 1978).

This study aims to assess the prospectivity on a continental scale for two magmatic-related U systems: intrusive- and volcanic-related. The results are presented in two accompanying maps (Schofield, 2010a; 2010b). The primary goal is to identify those igneous events and units which indicate the greatest potential for the presence of magmatic-related U systems. This is intended to form the basis for subsequent regional-scale assessments using detailed local or regional datasets, such as that undertaken for northern Queensland (Huston, 2010).

PROSPECTIVITY ANALYSIS METHODOLOGY

Broadly speaking, there are two general groups of approaches: empirical and conceptual (Knox-Robinson and Wyborn, 1997). Empirical methods are most readily applied to regions with numerous known deposits, with prospectivity criteria developed on the observed geological and spatial relationships. Conceptual approaches on the other hand are best suited to areas where there are insufficient known deposits with which to develop criteria. In the latter approach, prospectivity criteria are developed based on a mineral systems model, which translates key mineralising processes into mappable geoscientific criteria.

Employing a mineral systems model has several advantages. In contrast to the highly localised factors determined at the mine-scale, the geological processes underpinning a mineral system are mappable at large scales (Knox-Robinson and Wyborn, 1997). Most importantly, by using criteria based on process rather than relationship to known mineralisation, an assessment is able to be made of the prospectivity in relatively ‘greenfield’ areas. For this reason, a conceptual mineral system-based methodology is adopted for this investigation.

This study employs a mineral systems approach which has been modified from the 'Five Questions' developed by the Predictive Mineral Discovery Cooperative Research Centre (Walshe et al., 2005; Barnicoat, 2007). The Five Questions are: (1) What are the geodynamic and P-T histories of the system?; (2) What is the structural and lithological architecture of the system?; (3) What and where are fluid reservoirs and metal sources for the mineral system?; (4) What are the fluid flow drivers and pathways?; and (5) What are the metal (and ligand) transport and depositional processes?

The approach used in this study (Figure 1) consists of three components: (1) melt generation, (2) U concentration processes, and (3) U depositional processes. Melt generation is most closely related to question 1 of the Five Questions, since the geodynamic setting controls the type of melt which will be produced. This component deals most specifically with the source magma in magmatic-related systems. Uranium concentration incorporates processes responsible for enabling an igneous body to act as a metal source, which typically takes place via magmatic evolution processes. Thus U concentration processes are equivalent to question 3 of the Five Questions. As the melt evolves, ligand concentrations may also increase, and a magmatic fluid may be exsolved. The final component of the mineral systems model presented here are U depositional processes. In magmatic-related systems, U deposition may occur via a range of potential options (see below), and ligand and U behaviour may be strongly linked. Uranium depositional processes correspond to question 5 of the Five Questions.

These processes have been translated into mappable criteria, which are discussed below. Rather than actively mapping the processes themselves, the focus has been on mapping the products of these processes. For example, although anorogenic tectonic settings are important to the generation of A-type magmas for intrusive-related U systems, the distribution of A-type igneous units has been mapped instead, since these represent the product of the targeted process.

This mineral systems framework has been developed specifically for the purposes of this study, and thus not all of the Five Questions have a direct corresponding component. For instance, no criteria relating to fluid flow (question 4) have been developed for this continental scale study, since this must be assessed on a regional basis. Similarly, questions of architecture (question 2) have not been addressed, even though U-rich magma source regions and the distribution of permeable volcanic horizons may be useful. It is however not possible to constrain these without detailed knowledge of the stratigraphy of the regions in question.

INTEGRATION OF PROSPECTIVITY CRITERIA

Within the two general groups of prospectivity methods mentioned above, there are several different techniques which have been proposed for undertaking prospectivity analysis. These range from simple Boolean methods to more sophisticated Bayesian approaches (Bonham-Carter, 1995). Other workers have employed probabilistic methods encompassing both geological and economic considerations (for example, see Kreuzer et al., 2008). Common to all approaches is the collation and combination of favourable geoscientific criteria. Each method offers a differing approach to weighting and combining the criteria to produce the final map of predicted prospectivity. For this study a fuzzy logic approach has been used in preference to other techniques. A fuzzy logic approach balances the ability to capture uncertainty and incomplete data while also being relatively easy to implement.

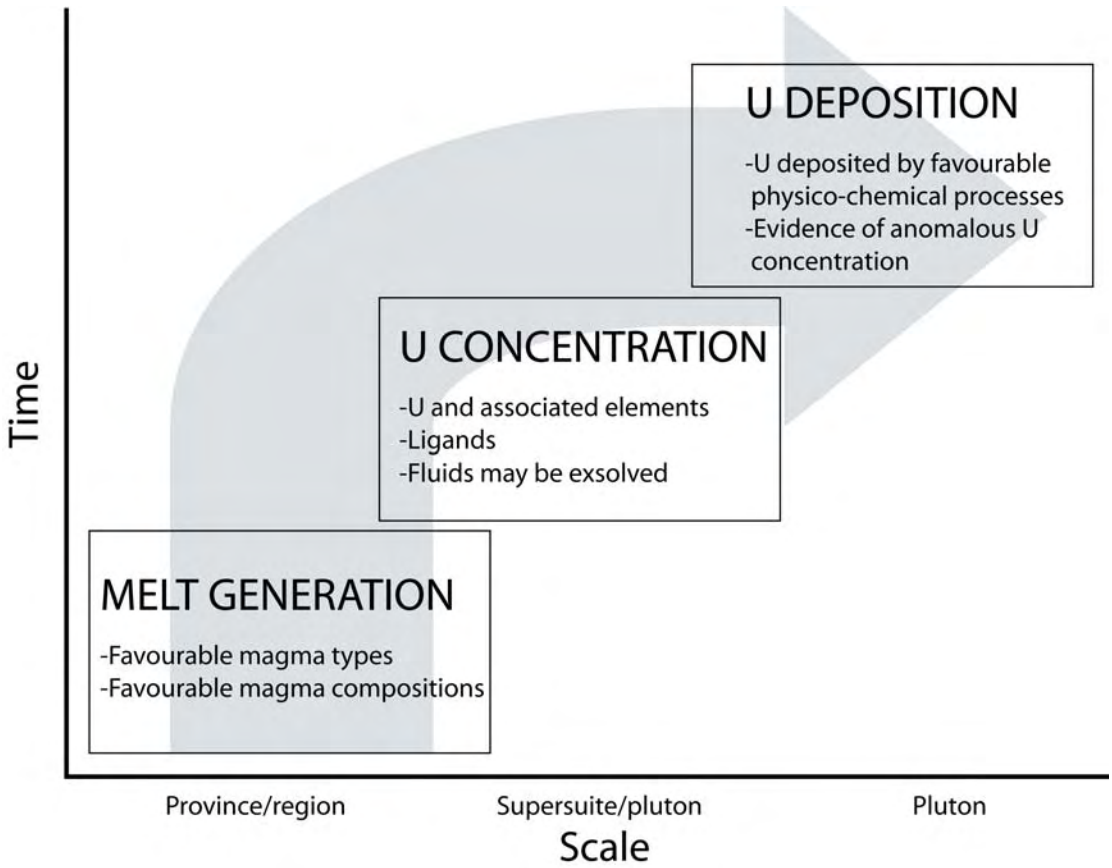

Figure 1: *Generalised mineral systems model used to assess the potential for magmatic-related U systems. There is a general progressive evolution of components in terms of time and scale, as shown by the grey arrow. The scale shown here corresponds to intrusive-related systems, but is also applicable to volcanic equivalents.*

The fuzzy logic approach

The fuzzy logic approach is based on the fuzzy set theory proposed by Zadeh (1965). Unlike conventional set theory, where membership values are based on a binary system (that is, 1 or 0), fuzzy membership values are defined as a continuous spectrum of values between 0 and 1. This is better suited to geological situations, where a level of uncertainty is common. The usefulness of this approach may be illustrated by considering bulk composition in magmatic-related U systems, where felsic magmas are an important criterion for prospectivity. In typical Boolean analysis using conventional set theory, a felsic igneous unit would receive a membership value of 1 (full membership), while mafic units would receive 0 (non-membership). A unit of mixed composition (that is, a unit with both felsic and mafic components) may receive a value of 0, ruling it unprospective, or 1, ruling it fully prospective. Neither of these possibilities satisfactorily reflects that the felsic rocks provide some degree of prospectivity, which is somewhat reduced by the mafic members. Using fuzzy set theory, the mixed unit may receive a fuzzy membership value of 0.5 in order to reflect the presence, but not dominance, of the felsic component.

Fuzzy membership values may be expressed as both discrete maps (such as geological unit polygons), or as a continuous values depicted as raster images, with the choice of values based on the subjective judgement of the analyst (Bonham-Carter, 1995; Knox-Robinson and Wyborn, 1997). Fuzzy membership values are not identical to probabilities, and different criteria should also be assigned fuzzy membership values relative to each other. That is, the maximum fuzzy membership value assigned for a given criterion must reflect its interpreted relative importance in the mineral system model. Once the datasets have been compiled and processed, prospectivity criteria are combined using one or more of five fuzzy operators (Table 1). A generalised workflow highlighting the main stages of this study is shown in Figure 2.

Table 1: Fuzzy operators used in the assessment for magmatic-related U systems.

OPERATOR	EQUATION	DESCRIPTION
Fuzzy AND	$\mu_{\text{combination}} = \text{MIN}(\mu_A, \mu_B, \mu_C, \ldots)$	Minimum operator
Fuzzy OR	$\mu_{\text{combination}} = \text{MAX}(\mu_A, \mu_B, \mu_C, \ldots)$	Maximum operator
Fuzzy algebraic product	$\mu_{\text{combination}} = \prod_{i=1}^{n} \mu_i$	Results ≤ smallest contributing value
Fuzzy algebraic sum	$\mu_{\text{combination}} = 1 - \prod_{i=1}^{n} (1-\mu)_i$	Results ≥ smallest contributing value
Gamma	$\mu_{\text{combination}} = (\text{Algebraic sum})^{\gamma} \times (\text{Algebraic product})^{1-\gamma}$	Combines the fuzzy product and sum

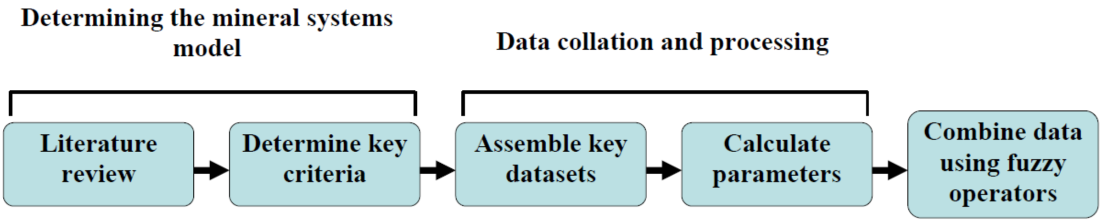

Figure 2: *Generalised workflow used during this study.*

DATASETS AND METHODS

Three primary datasets have been used during this investigation. These are Geoscience Australia's 1:1 000 000 national surface geology (Raymond et al., 2009) the radiometric maps of Australia (Minty et al., 2009), and whole rock geochemical data (for details see Schofield, 2009). Surface geology units have been classified according to whether they are intrusive or extrusive, based on the lithological group field contained within that dataset. In some cases, geological polygons have both intrusive and extrusive components. Therefore, some volcanic rocks are unavoidably included in the analysis for intrusive-related systems, and vice-versa. All spatial and other data analysis undertaken in this study was performed using ESRI ArcGIS software.

Prospectivity criteria developed from geochemical data are calculated on samples with volatile-free SiO_2 contents in the felsic range (>63 wt.%), since these are the most favourable for magmatic-related U systems. Each of the geochemical criteria requires the identification of "high" values for chosen elements. This has been determined in a semi-quantitative manner based on percentile rank (see discussion of prospectivity analysis methodology for each system below for details). For the purposes of this study, element concentrations in the 70th percentile or higher were considered 'high', with fuzzy membership values increasing with higher percentiles. The significant number of 'no data' points was accounted for by assigning the calculated median as 'typical' concentration. These are assigned a fuzzy membership value of 0.25. The median abundance was selected rather than the mean, since the latter is influenced by outlying values (Figure 3).

Although fuzzy membership values are calculated on the geochemical data points themselves, the final prospectivity map is produced by attributing these values to the surface geology. This is performed by extracting the average value of each criterion for all data points belonging to a given unit.

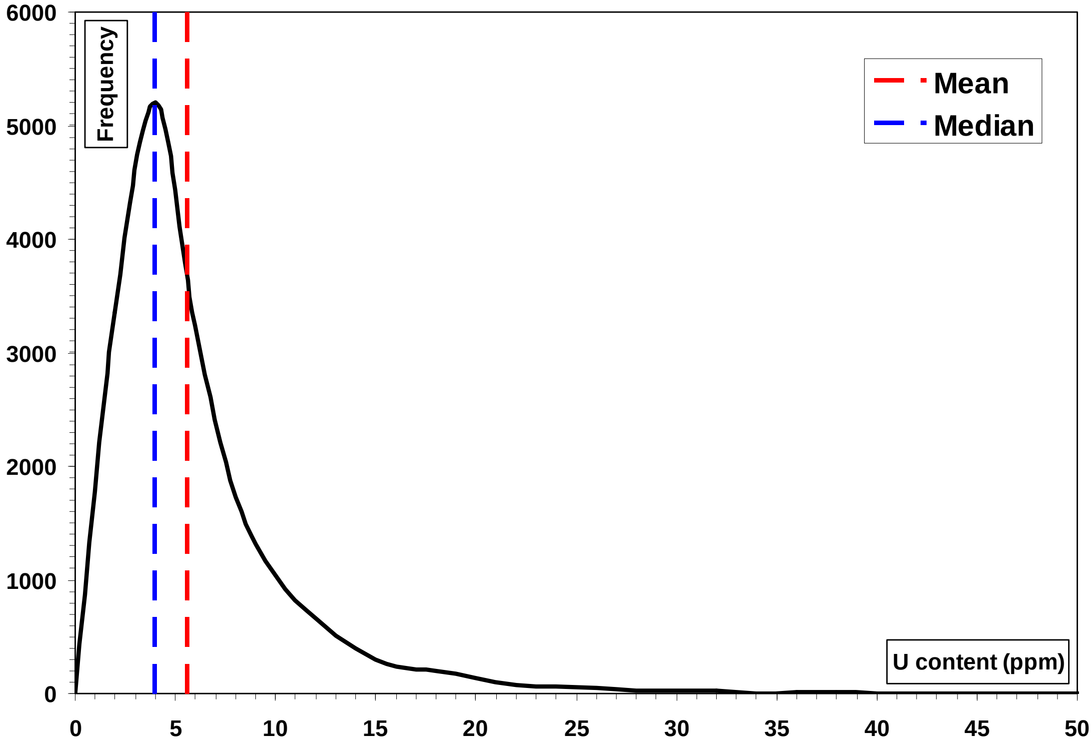

Figure 3: *Frequency plot for U content for intrusive-related samples derived from geochemistry. Note that the mean is skewed towards high values due to the non-normal distribution. The median on the other hand is a much better approximation of 'typical' values. Only U data in the 0-50 ppm range are shown.*

LIMITATIONS OF THIS STUDY

Attempting to assess prospectivity at such a broad scale has several attendant difficulties. Datasets used should ideally be consistent and continuous across the entire continent. This is why national datasets have been utilised, even though more detailed local datasets may exist. Development of prospectivity criteria for many of the processes involved in magmatic-related U systems require detailed datasets of the study area. Most notably, geological features suggesting the role of magmatic fluids (such as chemical alteration) are not captured in the datasets used. Furthermore, the volume of data is too great to permit rigorous quality control of the datasets. These limitations should be recognised when examining the results.

Summary of the behaviour of uranium in magmatic systems

A summary of the behaviour of U in magmatic systems is given by Skirrow et al. (2009), and hence only a brief discussion of the key features will be given here.

The U ion is highly incompatible in magmatic systems. Analyses of common mantle-derived magmas (N-MORB) show extremely low U abundances (0.047 ppm; Sun and McDonough, 1989). Ocean island basalts have U contents of 1.02 ppm (Sun and McDonough, 1989). Felsic igneous rocks on the other hand contain an average of 4.0 ppm (Rogers and Adams, 1969). Partial melting is therefore a process whereby U may be concentrated, although the residual source region of S-type melts may be higher in U than the melt product if U remains locked within refractory mineral phases such as zircon (Sawka and Chappell, 1986; 1987).

The importance of fractional crystallisation in generating very high U concentrations is well established. General trends show that sampled rocks with high U contents commonly have low Sr, and high Rb, which is consistent with the removal of feldspars from the melt. Other geochemical features, such as the K/Rb ratio, may also indicate that a high degree of fractional crystallisation has taken place. If however, the magma contains a large proportion of residual mineralogy brought up from the source region of the melt such as zircon, then U within the magma may be trapped by these phases. Uranium located in these residual phases is not available for fractional crystallisation.

Uranium does not readily substitute into the crystal lattice of the major rock forming minerals, such as feldspar and quartz, and is instead incorporated into a range of accessory mineral phases (Bea, 1996). The accessory mineralogy of the fractionating melt is sensitive to the physico-chemical conditions of the magma. Conditions which promote the crystallisation of U-poor phases, thereby increasing the concentration of U in the residual melt, are favourable for the genesis of igneous units with high U contents. For example, Cuney and Friedrich (1987) found that the crystallisation of uraninite is favoured in low-Ca peraluminous melts, since those conditions promote the crystallisation of monazite. This in turn concentrates U and lowers the Th/U ratio of the melt, thereby favouring uraninite.

Uranium may itself be incorporated into accessory mineral phases at a relatively early stage if the U solubility of the melt is low. High U solubilities are achieved when the melt is depolymerised via the production of non-bridging oxygens (NBOs; Farges et al., 1992). High Na+K/Al (peralkalinity) and halogens, especially F, are highly effective at producing NBOs, and hence enhance U solubility (Farges et al., 1992; Peiffert et al., 1994; Peiffert et al., 1996; Mysen et al., 2004). Therefore, fractional crystallisation in the presence of high alkali or halogen concentrations may lead to very high concentrations of U in the most differentiated magmas. Redox state and temperature may also increase U solubility, but the effect is minor compared with those mentioned above (Peiffert et al., 1994).

The partitioning of U between a silicate melt and a coexisting magmatic fluid is dependant upon the compositions of the fluid phase and the melt. The highest fluid/melt partition coefficients are achieved for peraluminous F-poor and Cl-rich melts, although significant U may partition into the fluid phase in other Cl- or F-rich fluids (Peiffert et al., 1994; Peiffert et al., 1996; see also discussion in Skirrow et al., 2009). Additionally, U may be leached from the igneous rock by a variety of fluids and concentrated, as has been suggested for the volcanic-related deposits of the Streltsovka Caldera (Chabiron et al., 2003).

The depositional mechanism for U in magmatic-related systems is problematic and poorly understood. Disseminated U hosted in magmatic-stage minerals is deposited via normal crystallisation of minerals from the melt. Suggestions for the depositional mechanism include fluid mixing, boiling, reduction and cooling (Skirrow et al., 2009). Other potential mechanisms may include pH change and decrease in the activity of ligands, such as decreased F activity due to the crystallisation of fluorite.

Intrusive-related uranium systems

Intrusive-related uranium systems appear to be uncommon globally. Two well known examples, the Ross Adams and Kvanefjeld deposits, will be briefly described here. Although perhaps the best known deposit associated with igneous rocks, the alaskite-hosted Rössing U deposit is not considered here, due to persisting uncertainties regarding the genesis of the deposit. The interpreted genetic model for U mineralisation at Rössing and the surrounding regions is related to the intrusion of Cambrian alaskitic pegmatites during the final stages of peak metamorphism (Kinnaird and Nex, 2007). Initial Sr isotope ratios indicate that these are crustally derived (Nex et al., 2002). Increasing U content is not correlated with other elements, which suggests that fractional crystallisation was not the mechanism for U enrichment (Nex et al., 2001; Kinnaird and Nex, 2007). However, this may also be due to post-magmatic disruption of primary U contents. Calculated zircon saturation temperatures reveal low magmatic temperatures (~675-700 degrees, McDermott et al., 1996).

The evidence given above has been interpreted to suggest that the U-rich alaskites in the Rössing area were produced via low degree partial melting of a uraniferous source region (for example, see Cuney and Kyser, 2008). At Rössing, U was remobilised and concentrated post-alaskite emplacement by fluids during the (?)Cretaceous, crystallising as secondary beta-uranophane (Nex et al., 2002). Although evidence suggests fractionation did not play a major role, the geochemical features of the alaskites are not dissimilar to strongly fractionated granites if a high degree of post-magmatic U redistribution is taken into account. Thus, several questions still remain regarding the Rössing deposit, especially regarding source region, U deposition and the genetic model. Therefore, Rössing-style mineralisation will not be targeted in this investigation.

THE ROSS ADAMS DEPOSIT

The Ross Adams deposit is genetically related to the Jurassic Bokan Mountain Granite Complex, which is situated on Prince of Wales Island, south-eastern Alaska, and was discovered in 1955 as a radiometric anomaly. 89,000 tonnes of ore have been mined from Bokan Mountain, predominately from the Ross Adams deposit (Cuney and Kyser, 2008). Ore at Ross Adams consists of uranothorite, uraninite and less than 2% sulphides (Thompson, 1988).

The Bokan Mountain Granite Complex is a multi-stage peralkaline ring dyke complex (Thompson et al., 1982). A U-Pb zircon age of 171±5 Ma has been obtained (De Saint-Andre et al., 1983), which differs somewhat from a whole-rock Rb-Sr age of 151±5 reported by Armstrong (1985). Twelve separate lithologies have been recognised, although riebeckite granite porphyry constitutes the dominant rock type (Thompson et al., 1982; Thompson, 1988). Ore is closely associated with albitised aegerine syenite, and forms pipe-like bodies along contacts, or as pods in shear zones (Thompson, 1988). An extensive network of fluorite-bearing veins extending up to 2.6 km from the eastern margin of the intrusion contains U-Th-REE mineralisation, with U grades of up to 2.8% (Staatz, 1978).

The Granite Complex is post-tectonic, and was emplaced at a shallow crustal depth (Thompson, 1988). As with many peralkaline granites, the ultimate magma source is thought to have been within the upper mantle (Thompson et al., 1982). Geochemically, the granites are characterised by high Na+K/Al, ranging from 0.9 to 2.08, with Na_2O>K_2O in all granite types (Thompson et al., 1982). Uranium content is only moderate, with an average of 12 ppm in unaltered granite (Cuney and Kyser, 2008).

The timing of mineralisation is closely associated with intrusion stage 2, which involved significant devolatilisation of the magma (Thompson et al., 1982; Thompson, 1988). Oxygen and carbon isotope analyses of hydrothermal calcite indicate that the fluids causing the alteration associated with mineralisation are of a magmatic origin (Thompson, 1988). The co-crystallisation of fluorite with calcite as an alteration mineral, fluorite-bearing veins, and the overall high F content of the magma strongly suggests that may have been important in transporting U as fluoro complexes. This fluid flow was concentrated in zones of structural weakness, such as zones of competency contrast and syn-magmatic faults. Uranium deposition may have occurred when these F complexes were destabilised.

THE KVANEFJELD DEPOSIT

The Middle Proterozoic Ilímaussaq alkaline igneous complex in southern Greenland forms part of the Gardar Igneous Province. Three major intrusive phases may be recognised, comprised of a number of exotic lithologies (for a summary of these, see Sørensen, 2001). These were emplaced at a shallow crustal level (2-3 km; Sørensen, 2001). The Kvanefjeld U deposit, discovered in 1956, is hosted by steenstrupine lujavrites of the Ilímaussaq alkaline complex (Nielsen and Steenfelt, 1979). Initial drilling in the 1970s identified 27 000 reasonably assured tonnes of U, mostly hosted by steenstrupine ($Na_{14}Ce_6Mn_2Fe_2(Zr, Th, U)(Si_6O_{18})_2(PO4)_7.3H2O$; Cuney and Kyser, 2008).

Bailey et al. (2001) provide a summary of the geochemistry of the Ilímaussaq alkaline complex. The most prominent features of the nepheline syenites, of which the lujavrites are part, are high Na+K/Al, high field strength elements (Zr, Hf, Nb, Ta, Th, U, Pb), rare earth elements, Sn, Li, Be, Rb, Zn, Sb, W, Mo, As and Ga, and low Ba, Sr, and transition metal elements (Co, Cu, Ni, Sc, V and Cr) except Zn.

The distinctive geochemical characteristics of the Ilímaussaq alkaline complex can be explained by extreme fractional crystallisation within a closed system (>99% fractionation; Bailey et al., 2001). The parental magma is thought to be an alkali basalt magma chamber deep in the crust, (Sørensen and Bailey, 2006). Basalts in the Ilímaussaq region contain higher alkalis, P, Ba, Sr, Nb and LREE than other basalts in the Gardar province, reflecting melting of an enriched mantle source (Sørensen, 2001). Such a source may also play an important role in the genesis of the Ross Adams deposit, as suggested by the presence of subduction-related alkali basalt magmatism preceding granite intrusion (Thompson et al., 1982).

MINERAL SYSTEMS MODEL FOR INTRUSIVE-RELATED URANIUM SYSTEMS

The mineral systems model for intrusive-related uranium systems is relatively simple, and is largely governed by well-known igneous processes. The two deposits described above are intimately associated with peralkaline magmatism originating from partial melting of the upper mantle followed by extreme fractional crystallisation. Although peralkaline rocks are some of the most prospective for intrusive-related U systems, other crustally-derived granite types, including high temperature I-type and A-type magmas, may also be highly prospective, as these are commonly high in U and F (Plant et al., 1999). The tectonic setting in which these magmas are generated and emplaced is typically anorogenic or extensional, but this may not be the case universally.

S-type granites, derived from partial melting of sedimentary or supracrustal rocks (Chappell and White, 2001), are considered to be comparatively unimportant in the genesis of intrusive-related U systems targeted in this study (Plant et al., 1999). This may be due to the melting of U-poor source rocks, U remaining in the granite source region (Sawka and Chappell, 1986; 1987) or, if magmatic temperature is low, a significant quantity of U being locked within restite phases (such as zircon; Chappell et al., 2000), thus rendering it unavailable to concentration with fractionation. While U-bearing alaskites at Rössing are interpreted to be derived from partial melting of sedimentary rocks (Berning et al., 1976; McDermott et al., 1996), the uncertainties mentioned above regarding this deposit prevent the development of a suitably robust mineral systems model.

The U content of the magma will be governed by the residual mineralogy in the source region and initial U concentration immediately following partial melting Elevated U concentration in the original melt is favoured where the source region is enriched, such as metasomatised mantle. Magmatic evolution processes, specifically fractional crystallisation, are critical in concentrating U in the melt as it ascends through the crust, and both the Bokan Mountain Granite Complex and Ilímaussaq intrusions have been highly fractionated, with U more highly concentrated in the most differentiated magmas. Although U is largely incompatible in the structure of the main rock forming minerals, and hence is concentrated with their removal during fractionation, it is able to be accommodated into a wide range of accessory minerals, such as titanite, zircon and monazite in relatively low concentrations (Bea, 1996). High U solubilities within the melt prevent the early partitioning of U into accessory phases at an early stage.

A peralkaline bulk rock composition, such as that which characterises the Bokan Mountain and Ilímaussaq intrusions, is the most effective chemical mechanism for maintaining U solubility. Uranium solubility is also enhanced by high halogen contents (Peiffert et al., 1996). In cases where U solubility is extremely high, abundant uraninite will not form, and U may be partitioned into refractory minerals (Cuney and Kyser, 2008). These present metallurgical complications and extraction of U from such minerals may be difficult and costly.

Uranium may occur within disseminated U-rich minerals throughout an igneous body, or may be present within veins, such as the I and L vein system at Bokan Mountain (Staatz, 1978). Fractionation alone is unlikely to be sufficient to generate economic grades of U. Rather, fluid-mediated processes are probably extremely important, and examples of this style of U mineralisation show evidence of sub-solidus or later remobilisation of U. As discussed above, U may be transported by Cl- or F-rich magmatic-hydrothermal fluids. The precipitation of U from these fluids in veins presents a more favourable target for exploration, since these will be higher grade, and U may be easier to extract. Therefore, mineralisation may occur at some distance from the igneous body in a country rock host.

The mineral systems model used here for intrusive-related U systems is presented diagrammatically in Figure 4. Based on Figure 4 and the discussion above, the following features are considered characteristic of these mineral systems:

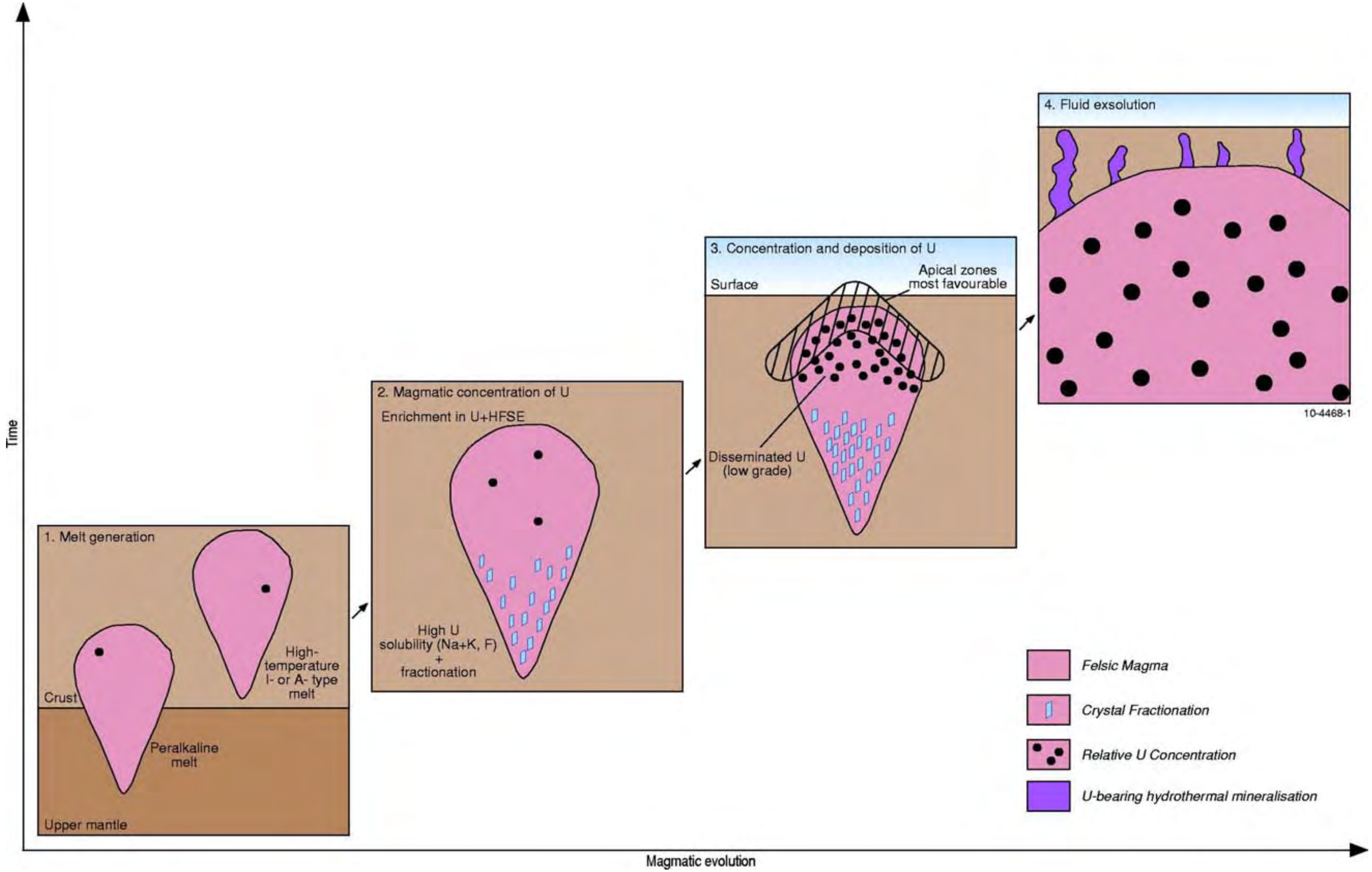

Figure 4: *Schematic illustration of the mineral systems model used for intrusive-related U systems.*

Source magma

The source magma component reflects the relative importance of certain magma types in the genesis of intrusive-related U deposits. Most often, these are of a broadly felsic composition, since mafic magmas are typically low in U (see above). Both the Bokan Mountain Granite Complex and the Ilímaussaq intrusions are characterised by a peralkaline bulk rock affinity. The high alkali contents of these magmas produce extremely high U solubilities, which in turn allow U to be strongly concentrated with fractional crystallisation. Hence, peralkaline igneous units are highly prospective, but are unfortunately uncommon in Australia.

As well as peralkaline magmas, some types of crustal melts are also prospective. These have the additional advantage of being sourced from material which has undergone a prior phase of U concentration. In particular, A- and I-type magmas may also have potential for generating magmatic-related U systems (see above). Prospectivity is enhanced when magmatic temperature is high, as this enables U-bearing minerals in the magma source region to be broken down, liberating U into the melt. High magmatic temperatures also slightly increases U solubility (Peiffert et al., 1994). To maintain high U solubility, non-peralkaline magmas require high concentrations of halogens.

The following criteria are considered important to this mineral systems component:
- The distribution of high temperature, high halogen A- or I-type magmas
- The distribution of peralkaline magmas
- The distribution of igneous rocks of a generally felsic composition

Uranium concentration processes

Magmatic concentration of U is facilitated most prominently by fractional crystallisation, and both the Ross Adams and Kvanefjeld U deposits are hosted by the extreme fractionation products of a parental magma. This process will manifest itself in high magmatic concentrations of U and other associated elements including, but not necessarily always, other HFSE. Since U is mobile under a range of conditions, and is therefore susceptible to be modified, observed concentrations are potentially not reflective of true values. An independent means of quantifying the level of enrichment of U and related elements may also be given by examining selected HFSE (Zr, Nb and Y) contents of a rock.

The following criteria are considered important to this mineral systems component:
- Geochemical indicators suggesting a high degree of fractional crystallisation has occurred
- High average U content
- High average content of high field strength elements (HFSE)

Uranium depositional processes

As discussed previously, the depositional mechanism of U in magmatic-related systems is poorly understood. In the absence of a firm understanding of process, direct evidence of anomalous U concentration may be used to highlight areas where U deposition has occurred. For this study, the following criterion is used:
- High U radiometric anomalies

PROSPECTIVITY ANALYSIS METHODOLOGY FOR INTRUSIVE-RELATED URANIUM SYSTEMS

The following section describes the methodology used to determine the prospectivity for intrusive-related U systems at a national scale. The final prospectivity map is a function of eight individual criteria maps, which will now be discussed.

Source magma

Intrusive composition

Intrusive geological units were extracted from the national surface geology dataset (Raymond et al., 2009) on the basis of their lithological group, as specified within the dataset. Fuzzy membership values based on their bulk composition (Table 2) were subjectively assigned and used to produce the compositional criterion map. Initial fuzzy membership values assigned were determined to have a disproportionate influence on the final prospectivity result for the relative importance of this criterion. The values were therefore adjusted using a scaling factor of 0.7. Although it is typically only felsic compositions which are prospective for intrusive-related U systems, low fuzzy membership values have also been assigned to intermediate compositions in order to allow for modest potential (for example, due to the presence of localised felsic differentiates).

Table 2: Fuzzy membership values assigned to intrusive rocks based on their composition. The initial fuzzy membership values assigned are shown in the second column. The final fuzzy membership values used are in the third column.

COMPOSITIONAL CLASS	FUZZY MEMBERSHIP VALUE 1	FUZZY MEMBERSHIP VALUE 2
Ultramafic to mafic	0.00	0.00
Intermediate to mafic	0.10	0.07
Unknown	0.10	0.07
Intermediate	0.25	0.18
Mixed (felsic to mafic)	0.50	0.35
Felsic to intermediate	0.70	0.49
Felsic	1.00	0.70

Magmatic affinity

Peralkaline rocks were attributed with a fuzzy membership value on the basis of their peralkalinity (that is, their Na+K/Al value). Due to the mobility of alkali elements under a range of conditions (see Rollinson, 1993 and references therein), a level of uncertainty is introduced, and fuzzy values are assigned for all samples with Na+K/Al > 0.95, with values greater than one having a fuzzy membership value of one. The relationship used to determine the specific fuzzy membership value is shown below in Figure 5. For non-peralkaline rocks, specific granite type was determined on the basis of geochemistry. The very limited number of samples which have been categorised as I-, S- or A-type necessitates the use of other approaches to determine granitoid type.

Whalen et al. (1987) proposed several discrimination diagrams to distinguish granitoids with an A-type affinity on the basis of their chemical composition. Three of these diagrams (Figure 6) have been used to assess the A-type character of individual geochemical analyses:
(1) 10 000Ga/Al versus Zr;
(2) Zr+Nb+Ce+Y versus Na_2O+K_2O/CaO; and
(3) 10 000Ga/Al versus Na_2O+K_2O/CaO.

Each geochemical sample was assessed against these discrimination diagrams to return a binary result (1 = positive A-type affinity, 0 = no affinity). The final probability was calculated as the number of positive results returned divided by three.

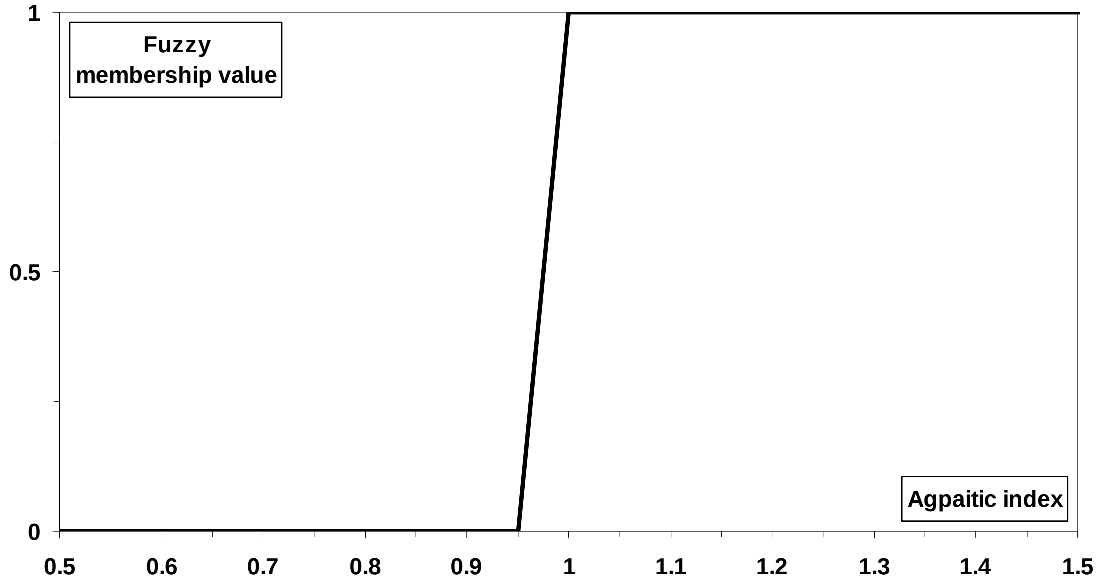

Figure 5: *Relationship defining the fuzzy membership value for peralkaline magmas. The steepness of the line does not reflect any relationship relating to U solubility. Rather, it is intended to account for potential analytical uncertainties.*

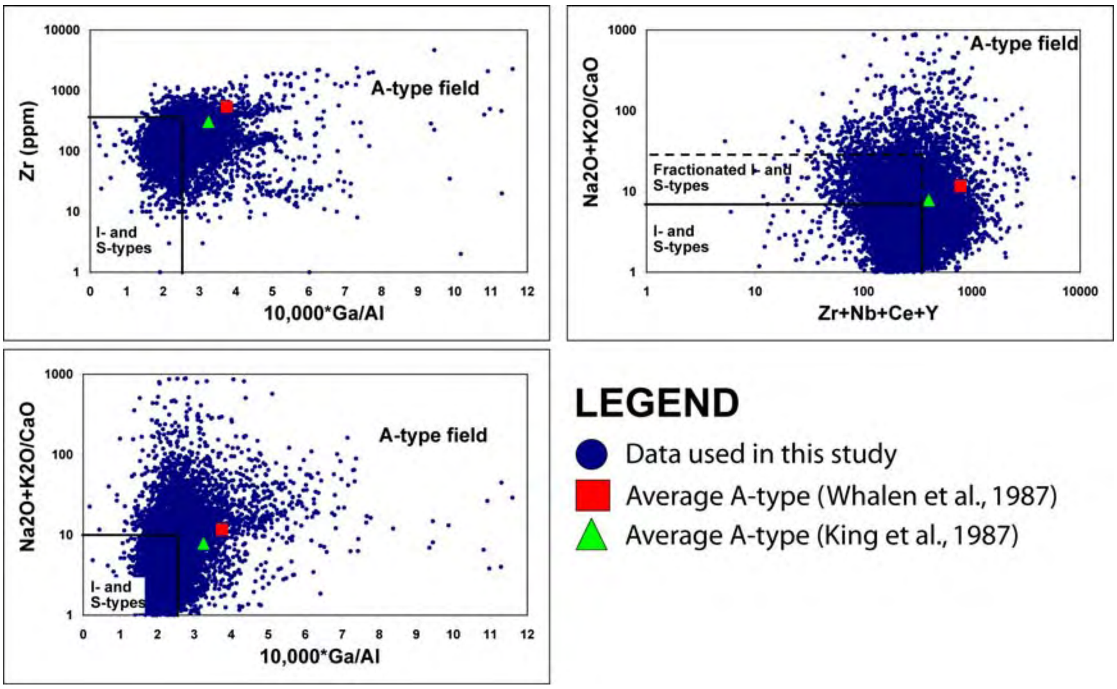

Figure 6: *A-type discrimination diagrams from Whalen et al. (1987) used in this report to determine A-type affinity. Average A-type compositions from Whalen et al. (1987) and King et al. (1997) are also shown.*

Classification of samples into I- and S-type affinities is more problematic. Criteria have been developed from Chappell and White (2001) to assign probabilities. These criteria are:

- Mineralogical: sample description contains "hornblende" (I-type).
- Normative mineralogy: I-type granitoids have normative diopside and <1% normative corundum, while S-type granitoids contain >1% normative corundum.
- Chemical: Samples with an aluminous saturation index (ASI) < 1.0 at SiO_2 contents less than 72 wt.% are classified as I-types, while an ASI>1.1 denotes an S-type.

While other criteria may be of use in the determination of classification type, the scale and scope of this study does not permit a more detailed analysis. In some cases, classification may be complicated by a number of factors. For example, weathering may strongly influence the calculated ASI. Nevertheless, the classification scheme presented above is deemed to be sufficient for the purposes of this investigation.

Fuzzy membership values were assigned by multiplying the assigned probabilities by the maximum value available (A- and I-type = 1.0, S-type = 0.2). These have been further modified by the magmatic temperature. Magmatic temperature is approximated by the zircon saturation temperature (T_{Zr}), which has been calculated according to Watson and Harrison (1983). Fuzzy membership values were then assigned to samples with T_{Zr}>650^{o}C by a linear function (Figure 7). For samples with insufficient data to calculate T_{Zr}, the modal T_{Zr} was attributed (775^{o}C). The fuzzy membership values for granitoid type and temperature were combined using the fuzzy algebraic product operator, since low magmatic temperature will decrease the potential of the rock.

Uranium solubility in non-peralkaline granites is strongly influenced by high halogen concentrations. While both Cl and F are able to increase U solubility, only F is considered here, due to the paucity of Cl data in the geochemistry used and the propensity of Cl to partition into the volatile phase, thus preventing representative determination of the actual Cl content of the magma. Furthermore, F is considered to perform a more important role than Cl in producing high U solubility (Peiffert et al., 1996). In peralkaline magmas, high alkali contents are significantly more important than halogens, and thus they are not considered for those magmas. To determine fuzzy membership values relating to F-enhanced U solubility, percentiles were calculated for the available F data, and assigned values (Table 3). Fuzzy membership values for F content were used to further modify the fuzzy membership value of non-peralkaline rocks by combining the two using the fuzzy algebraic sum operator. This operator has been used so as to increase the potential if high F is present, rather than decreasing it if it is not.

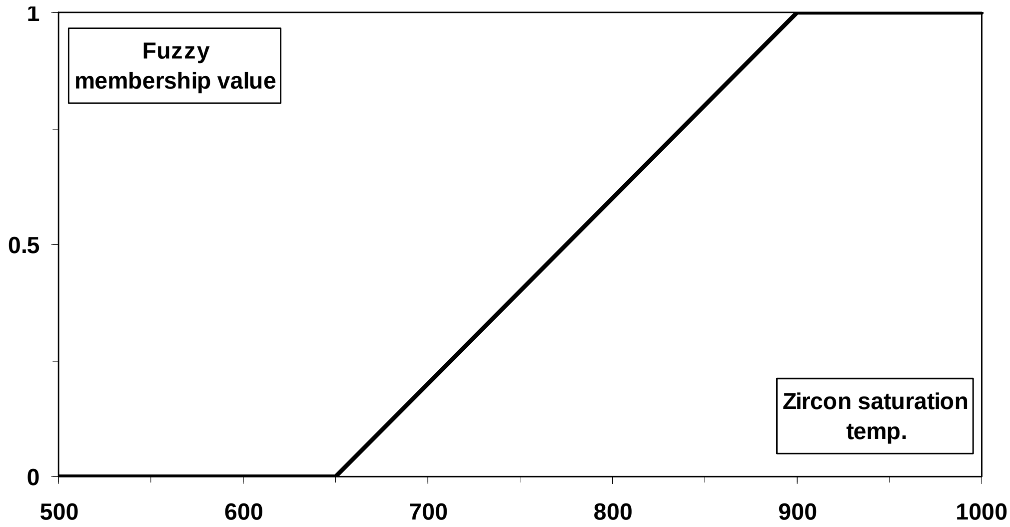

***Figure 7:** Relationship used to determine the fuzzy membership values for magmatic temperature.*

Uranium concentration processes

Fractional crystallisation

The Rb/Sr ratio is used to quantify the extent of fractional crystallisation. Changing Rb/Sr values reflect the removal of crystals (especially feldspar) from the melt, due to the differing compatibility of Sr (compatible) and Rb (incompatible). Thus, Rb/Sr will increase with progressive fractionation. A Rb/Sr value of 1.0 is selected as representing moderate fractionation, following Champion and Heinemann (1994). Samples with a Rb/Sr ratio of 10 or greater are considered to be highly fractionated. Fuzzy membership values were assigned according to the relationship shown in Figure 8. The Rb/Sr ratio may also change with other processes such as magma mixing, although it is not possible to determine the presence of this at the scale of this study.

High average uranium and high field strength element concentrations

Felsic intrusive units extracted from the national surface geology were attributed with a fuzzy membership value for their degree of U enrichment. Fuzzy membership values are given in Table 3. High field strength elements may also indicate a favourable igneous. Concentrations of Zr, Nb and Y, were assigned fuzzy membership values (Table 3), using the median as the cutoff value. The fuzzy algebraic product operator was used to combine HFSE data so that only the most HFSE-rich samples are given high fuzzy membership values.

Table 3: Thresholds and fuzzy membership values (FMV) used for calculating geochemical criteria for intrusive igneous rocks.

FMV	0	0.25	0.50	0.60	0.70	0.80	0.90	1.00
Percentile		Median	70 – 75	75 – 80	80 – 85	85 – 90	90 – 95	95 - 100
F (ppm)	<640	640	921	1034	1204	1504	1904	2719
U (ppm)	<4	4	6	7	8	9	11	15
Zr (ppm)	<155	155	194	209	225	250	291	382
Nb (ppm)	<10.5	10.5	14	15	17	20	24	32
Y (ppm)	<27	27	37	40	45	52	63	84

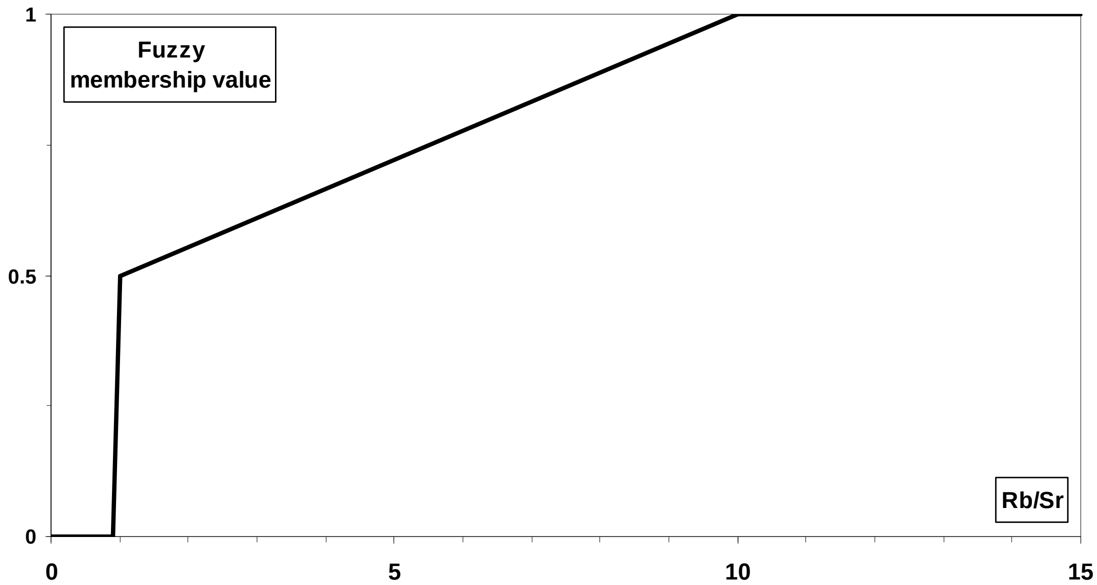

Figure 8: *Relationship defining the fuzzy membership value for fractional crystallisation. Sample with Rb/Sr ≥ 1 are moderately fractionated, and are assigned a value of 0.5. The steepness of the relationship between 0.8 and 1.0 is intended to allow samples with Rb/Sr just below 1 to be assigned a fuzzy membership value.*

Uranium deposition processes

High uranium radiometric anomalies

Uranium radiometric anomalies have been mapped using the airborne radiometric data from the radiometric map of Australia (Minty et al., 2009). The U^2/Th ratio has been selected for the analysis, as this may highlight areas of U enrichment. Statistics (mean and standard deviation) were calculated for each of the surface geology units based on stratigraphic number. U^2/Th values greater than one standard deviation above the mean for a given unit were assigned a fuzzy membership value of 0.6. Values greater than two standard deviations above the mean were given a fuzzy value of 0.8.

It is important to note that U values from airborne radiometrics are calculated from the measured radioactivity of various daughter products in the U decay series. As such, results may be skewed if disequilibrium effects are present. These will, however, only be of local significance. Another potential complication is high measured radioactivity in the vicinity of known U deposits which may record the locations of open pits or mine dumps, and not true anomalies.

COMBINING INTRUSIVE-RELATED DATA

Theoretically, prospectivity datasets may be combined using any of the fuzzy operators given in Table 1. For this study, most prospectivity assessments utilised the fuzzy gamma operation to combine the various criteria. Like the fuzzy algebraic sum and product operators, the fuzzy gamma operator takes into account all datasets. This is done by combining the fuzzy algebraic sum and product. A gamma value is used to give higher weighting to either the sum or product component of the operator. For example, combining the fuzzy membership values of 0.5 and 0.6 using a gamma value of 0.90 would be performed according to Equation 1. In practice, most mineral assessments utilise a gamma value greater than 0.90, to produce a greater final prospectivity result (Bonham-

Carter, 1995). To determine the optimal gamma value, gamma values in the range 0.90-0.95 and 0.98 were trialled. A value of 0.94 was eventually selected, since it highlights areas of potential, while not skewing the data too strongly towards high values (Figure 9).

$$[1-(1-0.5)\times(1-0.6)]^{0.90}\times[0.5\times0.6]^{0.10}=0.73 \qquad (Eq.1)$$

All of the prospectivity criteria were combined (Figure 10) using the selected gamma value, with the exception of the radiometric criterion. This was combined with the other criteria using the fuzzy algebraic sum operator. This was done so that areas in which a radiometric anomaly is absent are not unduly penalised. Thus, the radiometric criterion is viewed as the ‘icing’ on an already prospective intrusive ‘cake’, and the criterion is only applied to geological polygons which already have a prospectivity rating of 0.6 or higher.

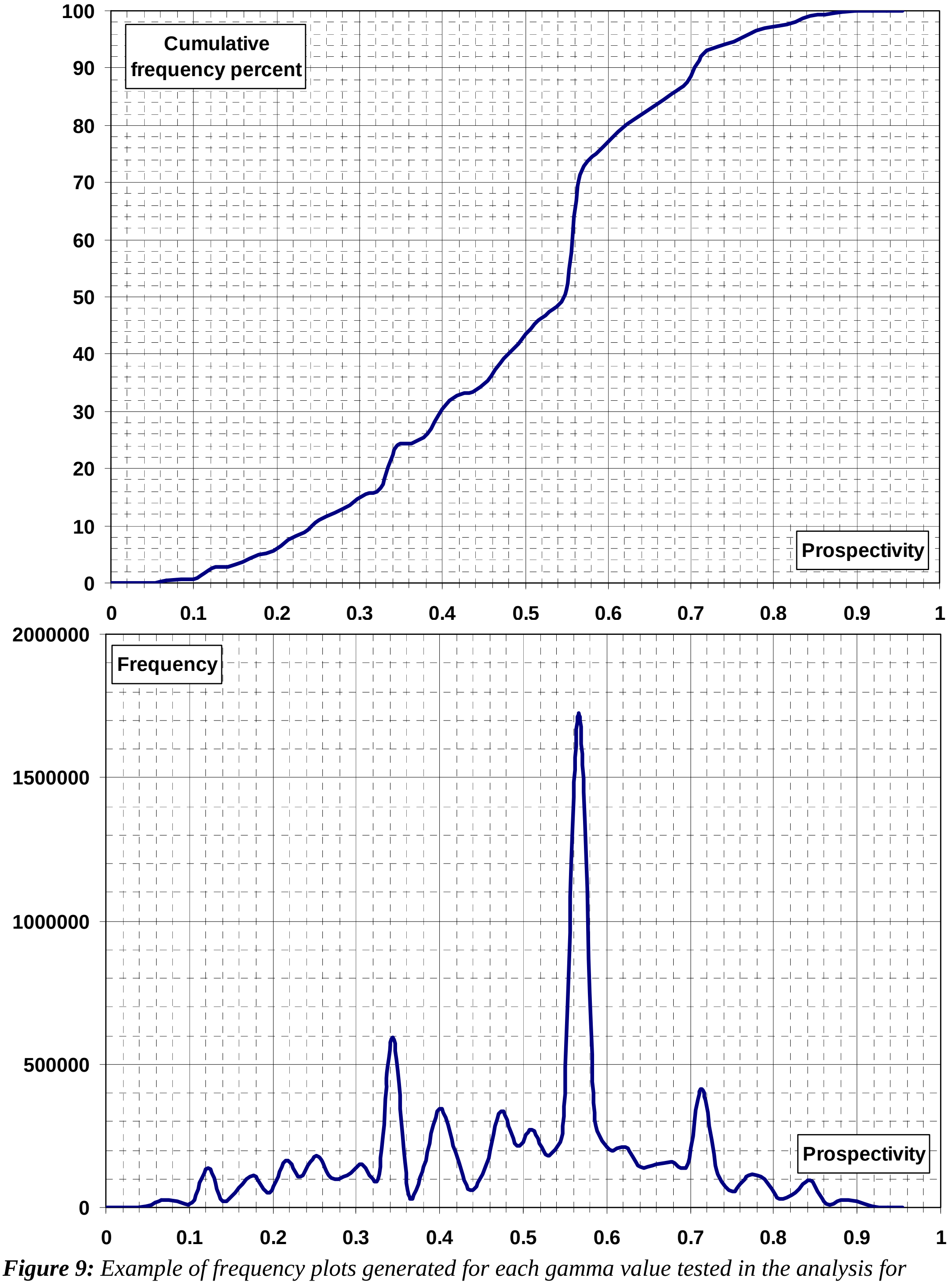

Figure 9: *Example of frequency plots generated for each gamma value tested in the analysis for intrusive-related U systems. The plots shown here correspond to a gamma value of 0.94. Graphs were generated by converting the polygon data to raster files using a 200 m cell size. Only polygons which contain data are plotted.*

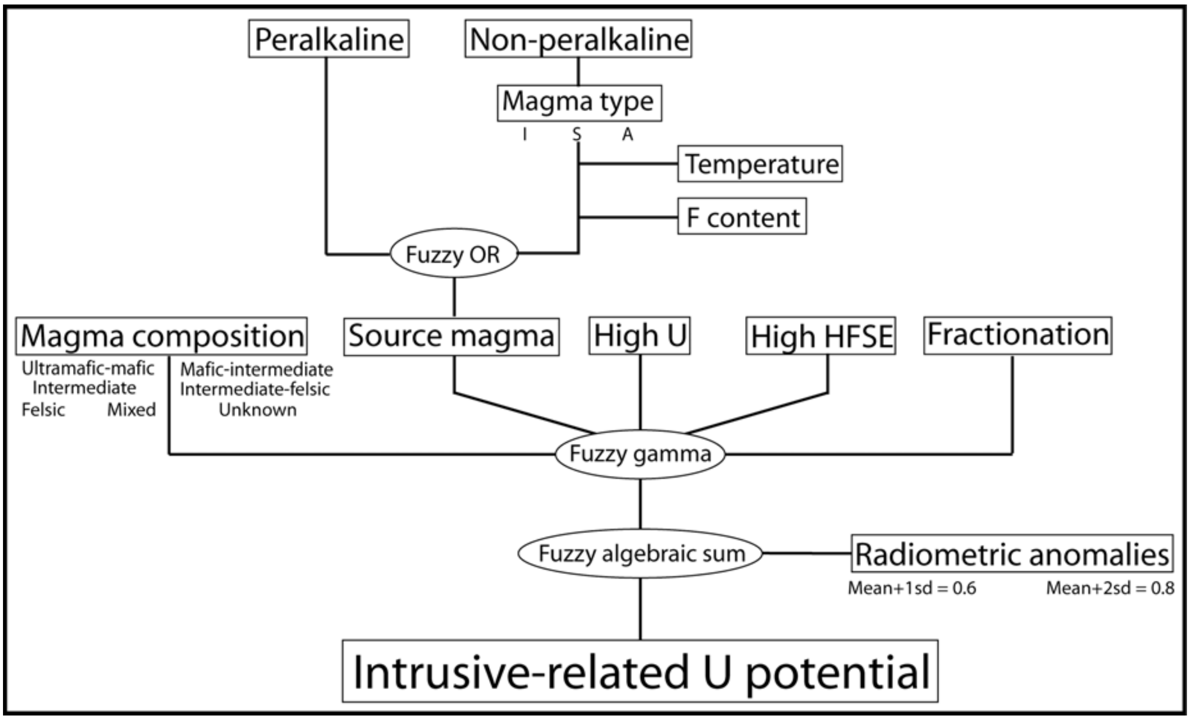

Figure 10: *Diagram showing the method for combining prospectivity criteria used in the assessment for intrusive-related systems. Note that not necessarily every fuzzy operator used has been shown. For details of these, refer to the text.*

Volcanic-related uranium systems

Volcanic-related U mineral systems are a significant deposit style worldwide, and may form very large world-class deposits. For example, deposits associated with the Late Jurassic Streltsovka Caldera in eastern Russia (representing the largest U field associated with volcanics in the world) have a total U resource exceeding 232 000 tonnes across 18 deposits (Laverov et al., 1992, cited in Cuney and Kyser, 2008). Other examples of U mineralisation associated with volcanism include the Sierra Pena Blanca district in Mexico (George-Aniel et al., 1991), the Marysvale Volcanic Field in Utah (Cunningham et al., 1994), and numerous deposits and prospects in Nevada and Oregon (Castor and Henry, 2000). In Australia, a number of deposits associated (at least spatially) with volcanics are known to occur in the Georgetown – Cairns area of northern Queensland (McKay and Miezitis, 2001). While these have traditionally been interpreted as volcanic-related, recent work suggests that they are more similar to unconformity-related systems (Wall, 2006; Matheson and Hurtig, 2009), and hence they will not be considered here in detail.

Mineralisation is typically associated with rhyolitic rocks, although the volcanic package may be bimodal and include sedimentary rocks. For example, the caldera fill at Streltsovka consists of basalt, andesite, trachydacite and rhyolite interlayered with sediments (Chabiron et al., 2001). Magma chemistry is probably extremely important, especially with respect to U solubility. The rhyolites which comprise 30-35% of the volcanic pile at Streltsovka (corresponding to a thickness of 50-100 m across the caldera) are characterised by a peralkaline bulk rock composition (Na+K/Al = 1.04 – 1.10) and extremely high F (1.4 – 2.7 wt.%; Chabiron et al., 2001). Using the experimental data of Peiffert et al. (1996), Chabiron et al. (2003) calculated that the Streltsovka rhyolites are strongly undersaturated with respect to U, and could theoretically accommodate up to 1.1 wt.%.

Coupled with indicators of a high degree of fractionation (Chabiron et al., 2001), high solubilities ensured that U was strongly concentrated in the residual melt fraction with progressive magmatic evolution. Similar chemistry is also observed in volcanic rocks associated with U mineralisation in Mexico and the United States.

Fission track studies indicate that at Streltsovka, U within the original rhyolite is almost entirely associated with the glassy matrix, which comprises 85-90% of the rock (Chabiron et al., 2003). This renders the U highly available to leaching, and is consistent with the significantly lower U content in altered bulk rock samples in comparison with unaltered melt inclusions (Chabiron et al., 2001). Mass balance calculations presented by Chabiron et al. (2003) suggest that around 300 000 tonnes of U may have been leached from the rhyolites across the caldera. In the Sierra Pena Blanca district, fission track studies indicate that the matrix of the Nopal rhyolite, corresponding to about 70% of the rock, contains 8 ppm U (George-Aniel et al., 1991). Analyses indicate that during alteration, U was leached, while Th and REE remained immobile, suggesting that U has been removed from the glassy matrix, while other associated elements remained within accessory mineral phases. Leaching and concentration of U from the igneous body is therefore a fundamental factor in the formation of volcanic-related deposits.

It is very unlikely that U mineralisation in volcanic-related systems is primary. Mineralisation is typically associated with hydrothermal alteration, and is well demonstrated at Streltsovka. The final phase of rhyolite eruption has been dated at 142±7 Ma (Chernyshev and Golubev, 1996). Phengite-illite ("hydromica") alteration, which immediately precedes the main phase of mineralisation, is dated at 133±5 Ma, which is identical with a U-Pb date age of 133±4 Ma obtained from ore-stage pitchblende (Chernyshev and Golubev, 1996). Thus, magmatism, hydrothermal alteration and mineralisation are all dated to within error of each other, indicating an important link relevant for volcanic-related mineral systems. A similar relationship has been observed in the Sierra Pena Blanca district, where kaolinite and montmorillonite alteration mineralogy characterise the alteration assemblage (George-Aniel et al., 1991), and in the Virgin Valley in Nevada (Cunningham et al., 1994). The strong localisation of U mineralisation within faults suggests that these acted as fluid conduits.

MINERAL SYSTEMS MODEL FOR VOLCANIC-RELATED URANIUM SYSTEMS

The discussion above provides important constraints on the mineral systems model used for prospectivity modelling for volcanic-related U systems. A first-order control on prospectivity is the distribution of felsic volcanic centres, and especially those associated with caldera complexes.

Uranium leaching by hydrothermal fluids is considered an essential component in the volcanic-related mineral systems model. Uranium hosted within refractory mineral phases, such as zircon, is difficult to liberate by hydrothermal fluids. In contrast, U hosted by volcanic glass or metamict minerals is highly susceptible to leaching. The magma chemistry and degree of magmatic evolution will strongly influence the primary distribution of U in the igneous rock. In terms of volcanic-related systems, a highly fractionated felsic extrusive with a high U solubility will crystallise U in a glassy matrix, thereby enabling U to be readily stripped out and re-concentrated. Such magmas will largely be highly alkaline and/or have high F contents.

The fluids responsible for the leaching and redeposition of U may be magmatic in origin, or, as suggested by Chabiron et al. (2003), may be of meteoric origin. In the latter case, fluid flow is driven by hydrothermal circulation cells established by the cooling melt. Faults, fractures or zones of rheological contrast act as fluid flow pathways and sites of U deposition, which may occur as a result of changes in pressure or temperature, changes in ligand activity, or other localised chemical control (Skirrow et al., 2009). Zones of clay and/or mica alteration may indicate locations of intense fluid flow. Alternatively, leaching and redeposition of U may occur post-volcanism (for example, due to meteoric fluids).

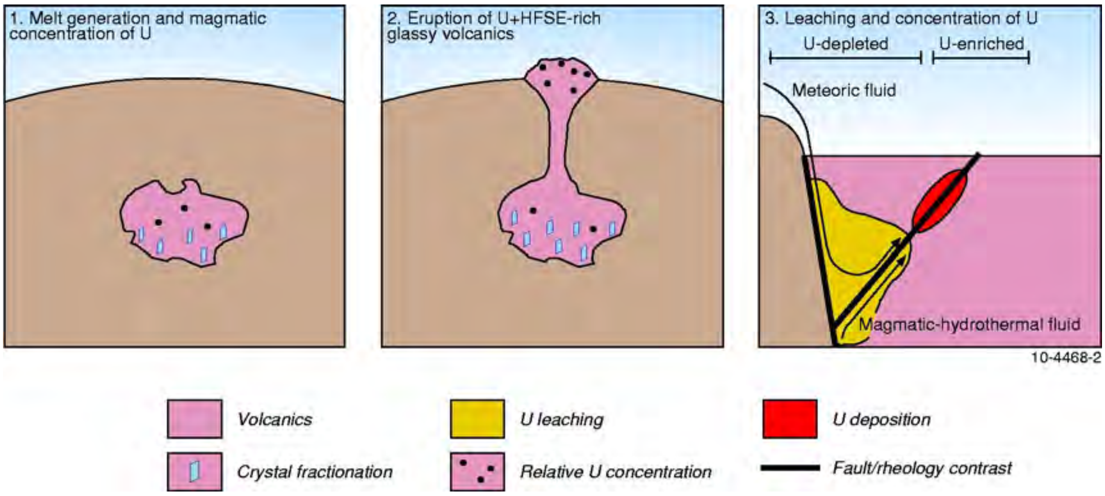

Figure 11: *Schematic illustration of the mineral systems model used for volcanic-related U systems.*

The mineral systems model used here for volcanic-related U systems is presented diagrammatically in Figure 11. Based on this and the discussion above, the following features are considered important for these mineral systems:

Source magma

Examples of U mineralisation associated with volcanic rocks typically occur in broadly felsic or alkaline rocks. High U solubility is essential for volcanic-related U systems, as this allows U to be concentrated with fractional crystallisation, and prevents incorporation of U into accessory mineral phases. If U solubility is very high, then saturation may never occur, and U will be partitioned into the glassy matrix, where it is able to be easily leached by hydrothermal fluids.

The following criteria are considered important to this mineral systems component:
- The distribution of volcanic rocks of a generally felsic or alkaline composition
- The distribution of volcanic units with potentially high U solubility due to high alkali (peralkaline) or halogen concentrations
- Rock descriptions suggesting availability of U to leaching (for example, glassy, ignimbritic)

Uranium concentration processes

Uranium is concentrated by fractional crystallisation during the magmatic phase. As with intrusive-related systems, magmatic-stage concentration of U may be manifest as high U and HFSE contents. Concentration of U via leaching and redeposition by hydrothermal fluids is interpreted to be an important process for volcanic-related U systems. Part of this process is encapsulated by the U availability criterion (see below). Other potentially favourable criteria include the presence of clay-mica alteration and fluid flow pathways (such as faults or rheological contrasts). It is not possible, however, to further constrain this process using the datasets employed for this study. These should be incorporated in subsequent analysis by using more detailed and additional data.

The following criteria are considered important to this mineral systems component:
- Geochemical indicators suggesting a high degree of fractional crystallisation has occurred
- Moderate-high average U content
- High average HFSE content

Uranium depositional processes

As with intrusive-related systems, defining mappable criteria for U depositional processes is not possible at this time, due to a lack of certainty regarding potential mechanisms. Regardless of the precise mechanism, zones of U enrichment may be mapped using radiometrics. Thus, the following criterion is considered important:
- High U radiometric anomalies.

PROSPECTIVITY ANALYSIS METHODOLOGY FOR VOLCANIC-RELATED URANIUM SYSTEMS

The following describes the methodology used to assess the prospectivity for volcanic-related U systems at a national scale. The volcanic-related system has many genetic similarities to the intrusive-related system discussed above, and hence there is significant overlap between the two. The final prospectivity map is a function of five individual criteria maps, which will now be discussed.

Source magma

Extrusive composition

Volcanic units were extracted from the surface geology and assigned a fuzzy membership value based on their composition. Values assigned are identical to those in Table 2.

Uranium solubility

High U solubility allows U to concentrate in the melt with progressive fractionation, and facilitates the partitioning of U into the glassy matrix. High U solubility may be produced by high alkali or halogen contents. Peralkaline rocks are the most favourable, and are associated with the examples described above. Although both Cl and F may assist in generating high U solubility, only F is considered due to the paucity of Cl data. The fuzzy membership value for peralkaline rocks is assigned according to Figure 5. Fuzzy membership values are assigned to F data on the basis of percentile rank according to Table 4.

Uranium availability

Leaching of U from a source of relatively normal U concentration and redeposition in more concentrated abundances in considered a crucial process in volcanic-related U systems. In order to incorporate this process into the prospectivity analysis, the national surface geology was interrogated for unit descriptions which suggest favourability for such processes. The descriptors used are:
- Glassy/vitric (fuzzy membership value = 0.8)
- Ignimbritic/tuffaceous (fuzzy membership value = 0.6)

Where no descriptor was found, a value of 0.2 was assigned.

Uranium concentration processes

Fractional crystallisation

As for the assessment for intrusive-related U systems, the degree of fractionation is quantified using the Rb/Sr ratio. The relationship shown in Figure 8 has been used to assign fuzzy membership values. For more details, refer to the discussion for intrusive-related U systems.

High average uranium and high field strength element concentrations

The degree of HFSE and U enrichment was calculated (Tables 4 and 5 respectively), and fuzzy membership values assigned. Because leaching of U is considered to be an important process in volcanic-related U systems, its contents may be disrupted (eg. Chabiron et al., 2001). As such, the fuzzy membership value assigned for U is lower than the equivalent value for intrusive-related systems. HFSE abundances on the other hand are probably a more reliable indicator.

Table 4: Thresholds and fuzzy membership values (FMV) used for calculating geochemical criteria for extrusive igneous rocks.

FMV	0	0.25	0.50	0.60	0.70	0.80	0.90	1.00
Percentile		Median	70 – 75	75 – 80	80 – 85	85 – 90	90 – 95	95 - 100
F (ppm)	<657	657	900	1000	1100	1300	1473	1800
Zr (ppm)	<213	213	300	330	372	420	495	640
Nb (ppm)	<12	12	16	19	22	26	30	46
Y (ppm)	<40	40	53	57	62	69	78	100

Table 5: Thresholds and fuzzy membership values for U contents of extrusive igneous rocks. Note that the percentile range for U differs to that used for other elements.

PERCENTILE		Median	70 - 80	80 - 90	90 - 95	95 - 100
CUTOFF (PPM)	<4.5	4.5	6	7	8	10
FMV	0	0.10	0.25	0.40	0.55	0.70

Uranium depositional processes

High uranium radiometric anomalies

Data presented by Chabiron et al. (2001) indicate that significant U was leached from the Streltsovka rhyolites, which is interpreted to represent a major metal source for the deposits (Chabiron et al., 2003). Locations of U enrichment were determined using the U^2/Th ratio calculated from radiometrics. This has been done in a manner identical to that used for the assessment for intrusive-related U systems, with the same fuzzy membership values employed.

COMBINING VOLCANIC-RELATED DATA

With the exception of high U and HFSE contents, and the radiometric criterion, all criteria in the volcanic-related U systems assessment were combined using the fuzzy gamma operator (Figure 12). Separate fuzzy membership values for U and HFSE content were combined using the fuzzy OR operator to create the U/HFSE element criterion. The fuzzy OR operator was used because the presence of either piece of evidence is favourable evidence for the presence of a mineral system, even though both may not necessarily be high. This differs somewhat from the methodology used for intrusive-related U systems.

A gamma value of 0.94 was selected to combine the data, as this highlights numerous potentially prospective areas, while not producing overwhelmingly high prospectivity (Figure 13). As for the analysis for intrusive-related U systems, the radiometric criterion was combined with the other criteria using the fuzzy algebraic sum operator.

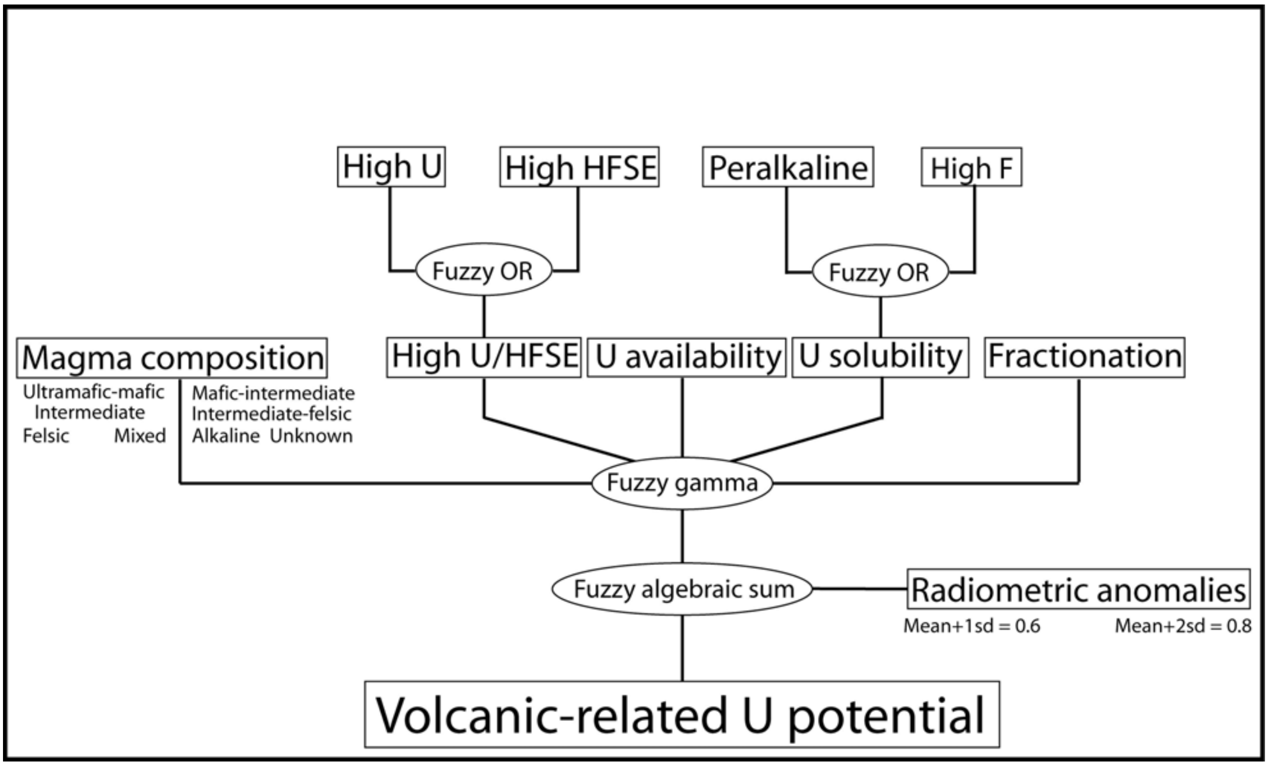

Figure 12: *Diagram showing the method for combining prospectivity criteria used in the assessment for volcanic-related systems.*

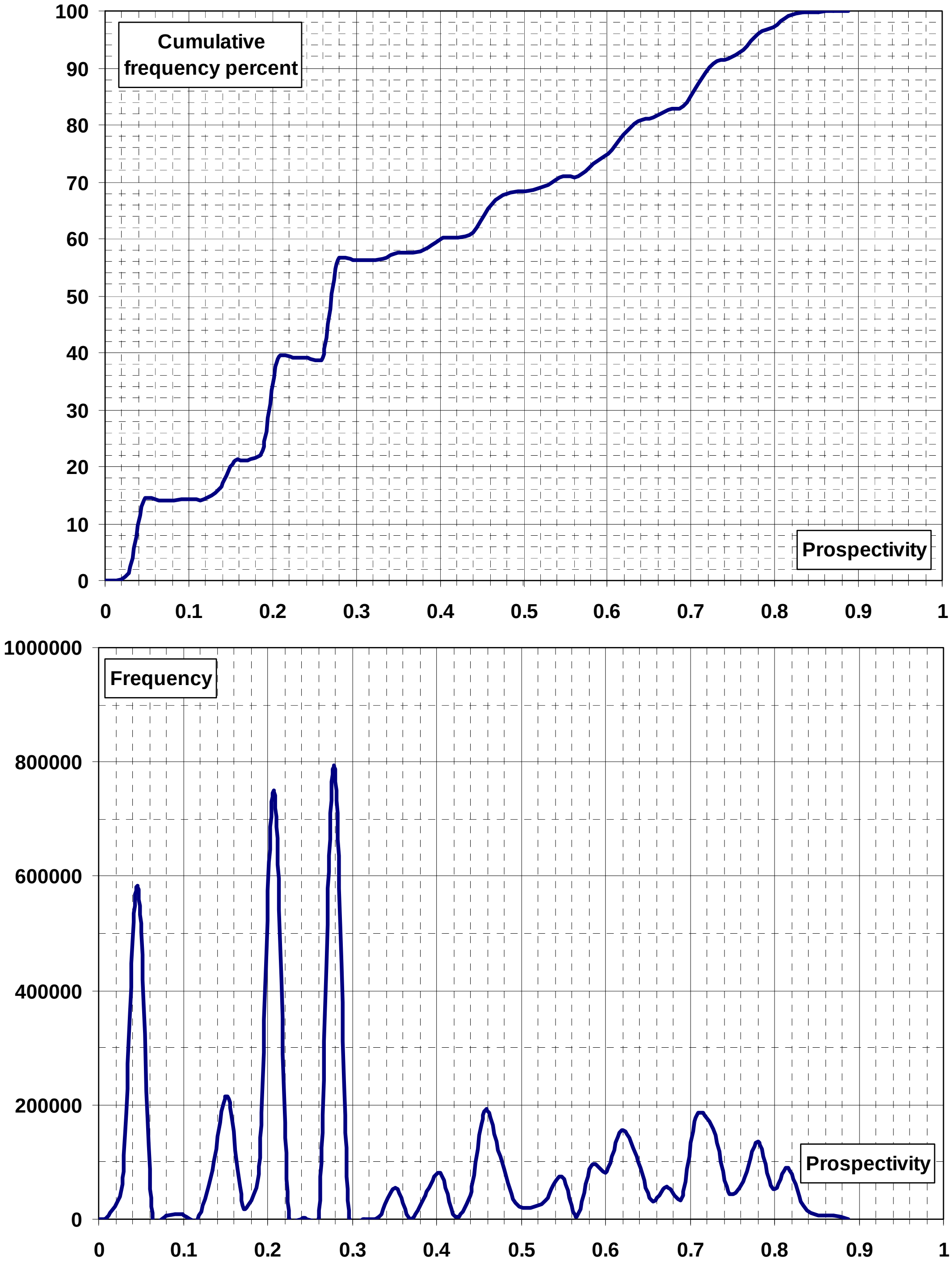

Figure 13: *Example of frequency plots generated for each gamma value tested in the analysis for volcanic-related U systems. The plots shown here correspond to a gamma value of 0.94. Graphs were generated by converting the polygon data to raster files using a 200 m cell size. Only polygons which contain data are plotted.*

Results

The discussion below will briefly outline those units which have the highest potential for intrusive-related U mineral systems. These results are also displayed in the accompanying maps for intrusive- and volcanic-related U systems (Schofield, 2010a; 2010b). Prospective units are ranked as either moderate-high (0.6-0.8) or high (>0.8). Present legislation in New South Wales, Victoria and Tasmania prohibits U exploration and/or mining, and furthermore these jurisdictions are not well known for U mineralisation. As such, only a brief discussion will be given of their potential. A full list of all units with medium-high or high prospectivity is given in Appendices 1 and 2. All unit names are extracted from the national surface geology dataset.

ANALYSIS OF INTRUSIVE-RELATED URANIUM PROSPECTIVITY

Intrusive igneous rocks showing potential for magmatic-related U systems occur throughout the continent. In many cases, these occur in already well-known U provinces, such as the Pine Creek, Mount Isa and Curnamona regions. In addition, this analysis has also highlighted high potential in areas which are not currently recognised as hosting significant U mineralisation. Most notable among these is the Arunta region in central Australia (Figure 14). The most prospective rocks in this region are the Paleoproterozoic Napperby Suite and Mesoproterozoic Southwark Suite on the northern margin of the Ngalia Basin, and the Paleoproterozoic Jinka Suite in the eastern Arunta region. Numerous units showing medium-high prospectivity are distributed throughout the region. For a full list of these, see Appendix 1. The northern Musgraves also exhibit unexpectedly high potential, especially in the Mesoproterozoic Hull Granite Suite. This region is currently not associated with any known U mineral occurrences. Units belonging to the Pitjantjatjara Supersuite have also been identified as having medium-high potential.

The Halls Creek-King Leopold region in Western Australia hosts the Oobagooma sandstone-hosted U deposit, as well as a small number of U mineral occurrences. Potential has also been identified for intrusive-related systems in the Paleoproterozoic Paperbark and Sally Downs Supersuites. Prospectivity is highest in components of the Paperbark Supersuite, with other units predominately having potential in the medium-high range. Felsic intrusives in the Archean cratons of Western Australia with potential for intrusive-related U systems include the Split Rock and Sisters Supersuites in the Pilbara Craton, and the extensive low-Ca granites in the Yilgarn Craton.

The Gascoyne region in Western Australia contains a large number of U mineral occurrences without any significant deposits, and pegmatite-hosted Rössing-style mineralisation has been identified just north of the Mortimer Hills (Carter, 1982). The Paleoproterozoic Durlacher Supersuite exhibits medium potential for intrusive-related U systems. Although overall potential is not exceedingly high, the identification of intrusives with medium prospectivity, numerous U mineral occurrences, and the known magmatic-related mineralisation suggest that the Gascoyne region is potentially prospective for intrusive-related U systems (Figure 15).

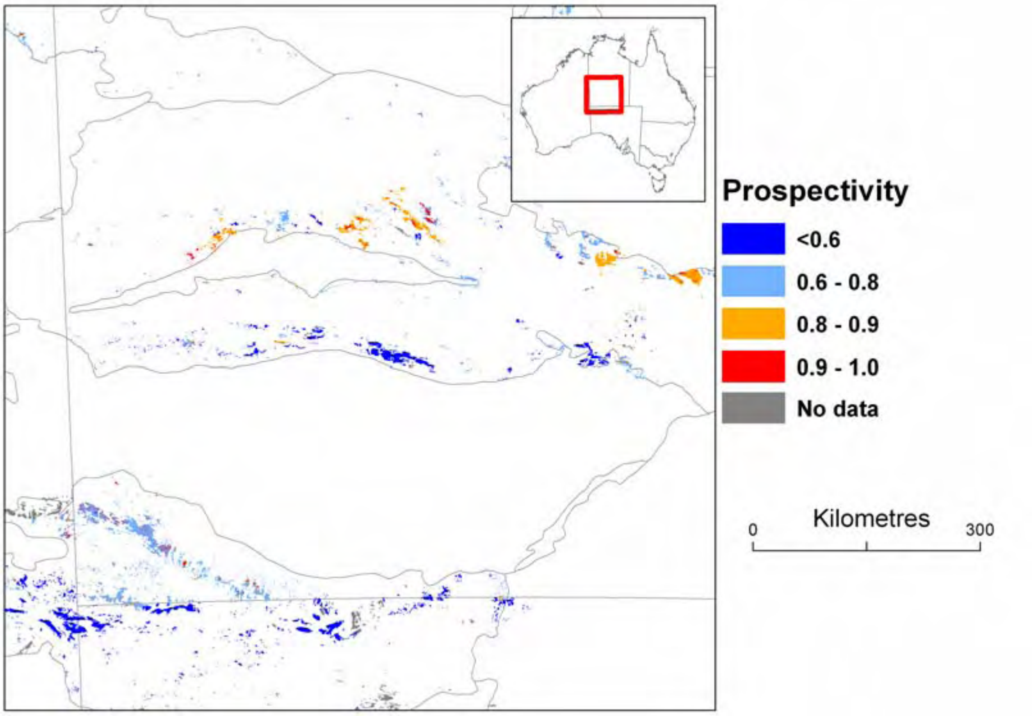

Figure 14: *Predicted prospectivity for intrusive-related U systems in the Arunta and northern Musgrave regions of the Northern Territory. Intrusive surface geology polygons are from the surface geology map of Australia (Raymond et al., 2009).*

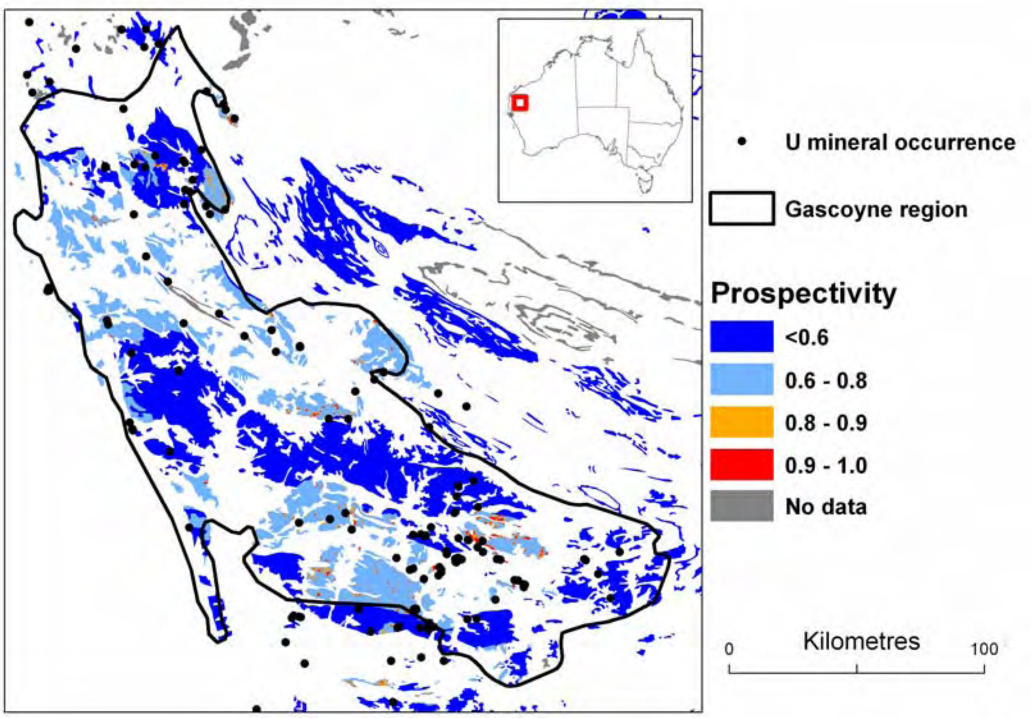

Figure 15: *Predicted prospectivity for intrusive-related U systems in the Gascoyne region. Although prospectivity is only in the medium-high range, the abundance of U mineral occurrences suggests that the potential for intrusive-related systems is high. Intrusive surface geology polygons are from the surface geology map of Australia (Raymond et al., 2009).*

Most of the known mineralisation associated with intrusive igneous rocks is confined to South Australia. The Crockers Well Granite, which is associated with a number of small deposits, is identified as having high potential in this analysis. Similarly, granites of the Mount Painter Inlier display very high prospectivity. These results assist in confirming the validity of the prospectivity analysis undertaken. As well as these areas of known prospectivity, the extensive Hiltaba Suite granitoids exhibit medium-high to high prospectivity across a large area of the Gawler Craton. The eastern Eyre Peninsula contains extensive granitoids of medium-high to high prospectivity, with the highest potential exhibited by the Donington Suite (referred to as the Younger Lincoln Supersuite in the surface geology dataset used).

In the known U provinces of Queensland (Mount Isa, Georgetown-Cairns and Murphy regions), high potential has been identified in Proterozoic and Phanerozoic intrusives. In the Mount Isa region, the Proterozoic Sybella Suite, Wonga-Burstall Suites and Williams Supersuite all display high potential. In northeastern Queensland (Georgetown-Cairns regions), Late Carboniferous granites of the extensive O'Briens Creek Supersuite, and to a lesser extent the Ootann Supersuite, are prospective. This region is already known for volcanic-related U mineralisation, and several small prospects related to intrusive igneous rocks are known (see Huston, 2010). These observations indicate that, as well as volcanic-related systems (see below), northeastern Queensland has high potential for intrusive-related U systems. The Murphy region on the Queensland-Northern Territory border is best known for unconformity-related U mineralisation. Potential has also been identified for intrusive-related U systems in the Paleoproterozoic Nicholson Granite Complex.

The Pine Creek region is another mature U province which exhibits high potential for intrusive-related U systems. In particular, the Paleoproterozoic Cullen Supersuite and David Suite exhibit medium-high and high prospectivity respectively.

Intrusive igneous rocks with medium-high or greater prospectivity rating are relatively widespread in the southeastern States. Many of these are related to the extensive Paleozoic magmatism in the Lachlan Fold Belt. Widespread medium-high prospectivity occurs across exposed granites in eastern New South Wales. The highest potential is found in the Narraburra Granite. Other units with high potential in New South Wales are the Doctor George Granite, Whipstick Adamellite, Obley Granite, Wangrah Suite, Mount Foster Monzonite, Jingo Creek Adamellite, Dandahra Creek Leucogranite and Boolahbone Granite. In Victoria, high potential has been identified in the Mount Leinster Igneous Complex. Potential in Victoria is otherwise medium-high. The most noteworthy granites in Tasmania belong to the Devonian Freycinet Suite in the eastern extremity of the State, where prospectivity is high. High potential also is found in northeastern Tasmania in the Heemskirk and Wombat Flat Granites, and in the Key Bay Granite near Flinders Island.

ANALYSIS OF VOLCANIC-RELATED URANIUM PROSPECTIVITY

Perhaps not surprisingly, the most prospective region in Australia for volcanic-related U systems is northern Queensland (Figure 16) which contains volcanic units with high U contents. The highest potential lies within the Georgetown-Cairns-Charters Towers regions. Potentially prospective units are mostly of a Carboniferous-Permian age, and include the Featherbed, Koolmoon, Mount Little, Newcastle Range and Scardons Volcanic Groups. In the western Georgetown region, volcanic rocks associated with the Mesoproterozoic Croydon Volcanic Group exhibit potential for volcanic-related U systems, and are not associated with known U mineral occurrences. Further to the south, near Emerald, high prospectivity has been identified in Cenozoic peralkaline rocks of the Peak Range and

Greybank Volcanics. To the west of the prospective volcanic rocks of the Georgetown-Cairns region, volcanic rocks in the Mount Isa region exhibit generally medium-high potential.

Prospectivity in South Australia is dominated by the voluminous Mesoproterozoic Gawler Range Volcanics. Prospectivity is typically in the medium-high range, although some units have been identified as highly prospective (Figure 17). The Gawler Range Volcanics are contemporaneous with the Hiltaba Suite granites. The medium-high prospectivity of the Hiltaba Suite for intrusive-related U systems, together with the medium-high to high potential of the Gawler Range Volcanics, indicates that the magmatic event which produced these igneous rocks is highly favourable for magmatic-related U systems. Thus, igneous rocks of this age should be regarded as prospective. Although U mineral occurrences are rare in the vicinity of the Gawler Range Volcanics, these results suggest that South Australia has significant potential for volcanic-related U systems.

In the Northern Territory, potential is greatest in the southern Pine Creek region. The Paleoproterozoic Pul Pul Rhyolite is identified as having the highest prospectivity. The Plum Tree Creek Volcanics are also prospective in the medium-high range. Volcanic units with potential for volcanic-related U systems have also been identified in regions which are currently poor in known U mineral occurrences. These include Paleoproterozoic volcanics of the Ooradidgee Group, which occur predominately in the Davenport region, but also extend into the northern Arunta and southern Tennant Creek Regions. The prospectivity of these volcanics ranges from medium-high to high.

Based on this analysis, prospectivity for volcanic-related U systems is lower in Western Australia than in other States and Territories in which exploration is currently permitted. As well as having potential for intrusive-related U systems, it is suggested that the Halls Creek-King Leopold region also has potential for volcanic-related U. The most favourable units have medium-high prospectivity, and belong to the Paleoproterozoic Koongie Park Formation.

Potential for volcanic-related U systems in the southeastern States is dominated by New South Wales. Phanerozoic volcanic rocks in central to southeastern New South Wales typically exhibit prospectivity in the medium-high range. Most notable are volcanics of the Wandsworth Volcanic Group, Douro Group and Kopyje Group. In Victoria, Silurian-Devonian volcanics of the Dartella Volcanic Group and Enano Group show medium-high potential. Tasmania is largely unprospective for volcanic-related U, with only the Tyndall Group of the Mount Read Volcanics exhibiting medium-high prospectivity. Volcanic units with high prospectivity ratings all occur in New South Wales, with the highest prospectivity in the Early Silurian Ina Volcanics.

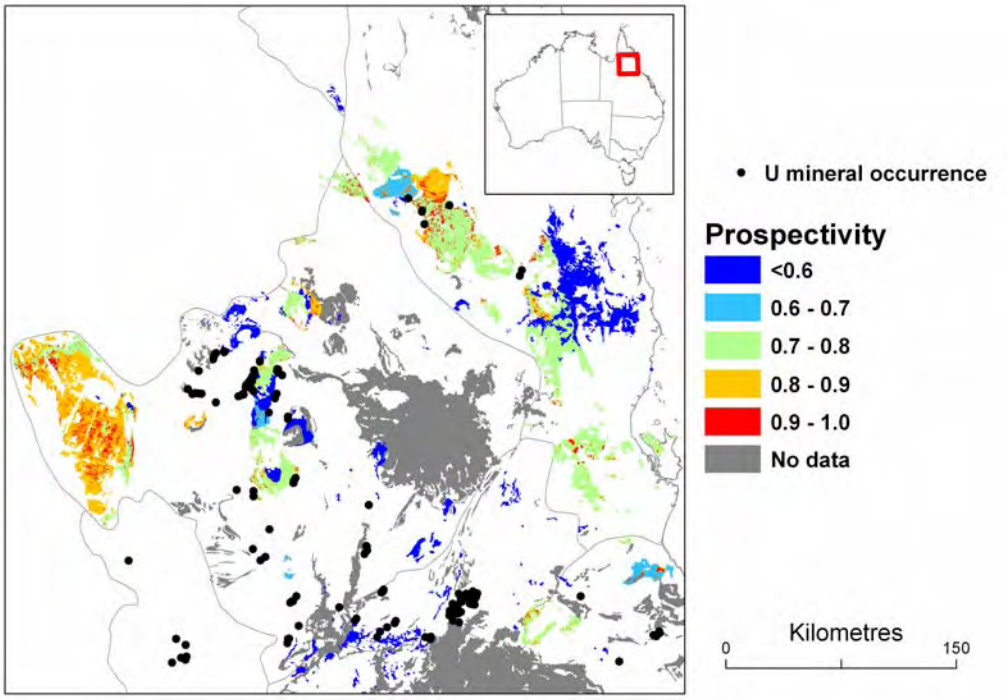

Figure 16: *Predicted prospectivity for volcanic-related U systems in the Georgetown-Cairns region. Volcanic surface geology polygons are from the surface geology map of Australia (Raymond et al., 2009).*

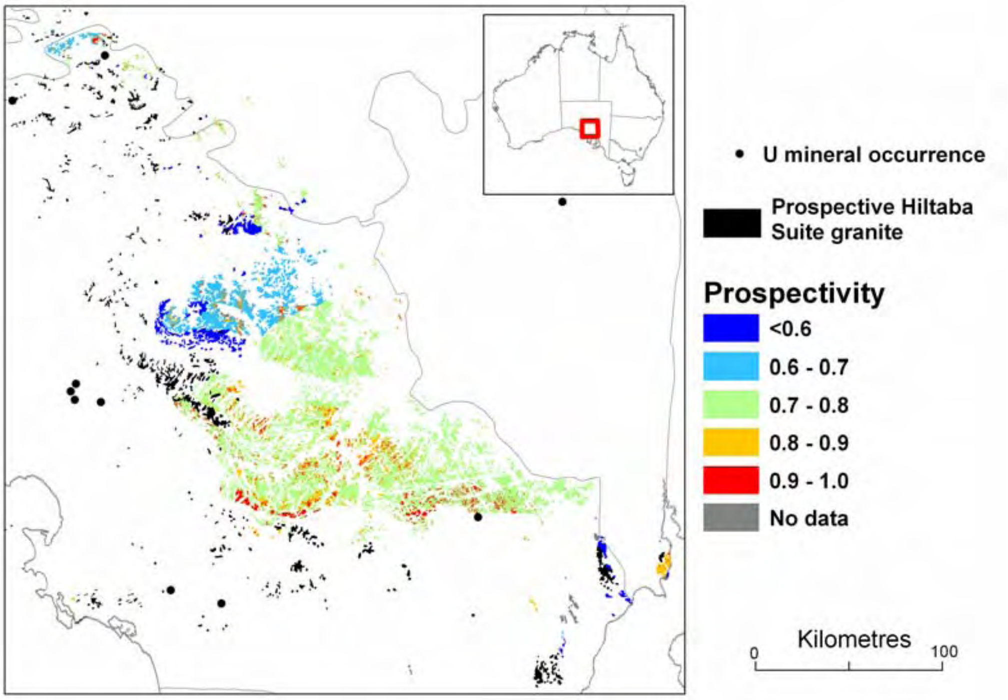

Figure 17: *Predicted prospectivity in the Gawler Range Volcanics of South Australia. Prospective units of the contemporaneous Hiltaba Suite granitoids are also plotted so as to demonstrate the high potential of this region for both intrusive- and extrusive-related U mineral systems. Volcanic surface geology polygons are from the surface geology map of Australia (Raymond et al., 2009).*

Conclusions and recommendations for future work

Although there are only minor known occurrences of magmatic-related U mineralisation, this study has shown that there is significant potential for unknown systems in igneous rocks across Australia. In many cases, igneous rocks showing high potential for intrusive- or volcanic-related U systems occur within provinces already well known for U mineralisation. While the U potential of these regions is already established, this investigation has demonstrated that potential occurs for U mineralisation different to that already known. For example, the Pine Creek region, although best known for its world-class unconformity-related U deposits, has been identified as prospective for both intrusive- and volcanic-related U systems. Similarly, potential for intrusive-related U systems is indicated by this study in the Georgetown-Cairns region, even though it is better known for U mineralisation associated with volcanics.

Potential for magmatic-related U systems has also been identified in regions which are not currently known as U provinces. Most notably, the analysis has highlighted central Australia as having significant potential for intrusive-related U systems. In particular, prospective units in the Arunta and northern Musgrave regions warrant further investigation. Likewise, the King Leopold-Halls Creek region in Western Australia has potential for both intrusive- and volcanic-related U mineralisation.

Based on the results of this investigation, the hypothesis that Australia is currently under-represented in the magmatic-related family of U mineral systems appears to be confirmed. The magmatic events and regions highlighted during this study provide the basis for subsequent follow-up work. In particular, the use of detailed local datasets in regional studies of areas of broadly identified potential will be essential. Potential zones of hydrothermal alteration and fluid flow pathways will greatly assist in better constraining the prospectivity for both intrusive- and volcanic-related U systems. Another valuable dataset, particularly in regard to volcanic-related U systems, is detailed petrographic descriptions of individual geological units. This would enable the location of U within the rock to be better understood, and allow for an assessment to be made of its susceptibility to concentration by hydrothermal fluids.

Opportunity also exists for developing mappable criteria corresponding to U depositional processes. The current understanding of the processes by which U is deposited in high temperature systems is poorly understood. If this could be better constrained, then a more rigorous assessment of potential sites of U deposition could be made, and the identification of prospective units further refined.

Acknowledgements

This report has greatly benefited from reviews by David Champion and Richard Chopping. The accompanying maps were produced with the assistance of Gerard Stewart. Roger Skirrow, Subhash Jaireth and Anthony Budd are thanked for their helpful input into the prospectivity analysis.

References

Armstrong, R. L., 1985. Rb–Sr dating of the Bokan Mountain granite complex and its country rocks. *Canadian Journal of Earth Sciences*, **22**, 1233-1236pp.

Bailey, J. C., Gwozdz, R., Rose-Hansen, J. and Sørensen, H., 2001. Geochemical overview of the Ilímaussaq alkaline complex, south Greenland. *Geology of Greenland Survey Bulletin*, **190**, 35-53pp.

Barnicoat, A. C., 2007. Mineral systems and exploration science: linking fundamental controls on ore deposition with the exploration process. *Digging Deeper: Proceedings of the Ninth Biennial SGA Meeting, Dublin*, 1407-1411pp.

Bea, F., 1996. Residence of REE, Y, Th and U in granites and crustal protoliths; implications for the chemistry of crustal melts. *Journal of Petrology*, **37**, 521-552pp.

Berning, J., Cooke, R., Hiemstra, S. A. and Hoffman, U., 1976. The Rössing uranium deposit, south west Africa. *Economic Geology*, **71**, 351-368pp.

Bonham-Carter, G. F., 1995. Geographic information systems for geoscientists: modelling with GIS. New York, Pergamon Press, 398p.

Carter, J. D., 1982. Mortimer Hills pegmatite uranium prospect: a Rossing-style uranium deposit in the Gascoyne Province. *Geological Survey of Western Australia Professional Papers. Report 12*, 27-31pp.

Castor, S. B. and Henry, C. D., 2000. Geology, geochemistry, and origin of volcanic rock-hosted uranium deposits in northwestern Nevada and southeastern Oregon, USA. *Ore Geology Reviews*, **16**, 1-40pp.

Chabiron, A., Alyoshin, A. P., Cuney, M., Deloule, E., Golubev, V. N., Velitchkin, V. I. and Poty, B., 2001. Geochemistry of the rhyolitic magmas from the Streltsovka caldera (Transbaikalia, Russia): a melt inclusion study. *Chemical Geology*, **175**, 273-290pp.

Chabiron, A., Cuney, M. and Poty, B., 2003. Possible uranium sources for the largest uranium district associated with volcanism: the Streltsovka caldera (Transbaikalia, Russia). *Mineralium Deposita*, **38**, 127-140pp.

Champion, D. C. and Heinemann, M. A., 1994. Igneous rocks of northern Queensland: 1:500 000 map and explanatory notes. *AGSO Record 1994/11*.

Chappell, B. W. and White, A. J. R., 2001. Two contrasting granite types: 25 years later. *Australian Journal of Earth Sciences*, **48**, 489-499pp.

Chappell, B. W., White, A. J. R., Williams, I. S., Wyborn, D. and Wyborn, L. A. I., 2000. Lachlan Fold Belt granites revisited: high- and low-temperature granites and their implications. *Australian Journal of Earth Sciences*, **47**, 123-138pp.

Chernyshev, I. V. and Golubev, V. N., 1996. The Strel'tsovkoe deposit, eastern Transbaikalia: isotope dating of mineralisation in Russia's largest uranium deposit (in Russian). **10**, 924-937pp.

Cowley, W. M., Katona, L. F. and Gouthas, G., 2009. Assessment of mineral prospectivity of the northern Flinders Ranges using GIS analysis. *PIRSA Report Book 2009/19*.

Cuney, M. and Friedrich, M., 1987. Physicochemical and crystal-chemical controls on accessory mineral paragenesis in granitoids: implications for uranium metallogenesis. *Bulletin de Mineralogie*, **110**, 235-247pp.

Cuney, M. and Kyser, K., 2008. Recent and not-so-recent developments in uranium deposits and implications for exploration. *Mineralogical Association of Canada Shortcourse Series, Quebec City*, **39**, 258pp.

Cunningham, C. G., Steven, T. A., Rowley, P. D., Naeser, C. W., Mehnert, H. H., Hedge, C. E. and Ludwig, K. R., 1994. Evolution of volcanic rocks and associated ore deposits in the Marysvale Volcanic Field, Utah. *Economic Geology*, **89**, 2003-2005pp.

De Saint-Andre, B., Lancelot, J. R. and Collot, B., 1983. U-Pb geochronology of the Bokan Mountain peralkaline granite, southeastern Alaska. *Canadian Journal of Earth Sciences*, **20**, 236-245pp.

Farges, F., Ponander, C. W., Calas, G. and Brown, G. E., 1992. Structural environments of incompatible elements in silicate glass/melt systems. II. U(IV), U(V), and U(VI). *Geochimica et Cosmochimica Acta*, **56**, 4205-4220pp.

George-Aniel, B., Leroy, J. L. and Poty, B., 1991. Volcanogenic uranium mineralizations in the Sierra Pena Blanca district, Chihuahua, Mexico: three genetic models. *Economic Geology*, **86**, 233-248pp.

Huston, D. L. (ed.), 2010. An assessment of the energy mineral and geothermal potential of north Queensland. *Geoscience Australia Record 2010/14*.

King, P. L., White, A. J. R., Chappell, B. W. and Allen, C. M., 1997. Characterization and origin of aluminous A-type granites from the Lachlan Fold Belt, southeastern Australia. *Journal of Petrology*, **38**, 371-391pp.

Kinnaird, J. A. and Nex, P. A. M., 2007. A review of geological controls on uranium mineralisation in sheeted leucogranites within the Damara Orogen, Namibia. *Applied Earth Sciences: IMM Transactions Section B*, **116**, 68-85pp.

Knox-Robinson, C. M. and Wyborn, L. A. I., 1997. Towards a holistic exploration strategy: using geographic information systems as a tool to enhance exploration. *Australian Journal of Earth Sciences*, **44**, 453-463pp.

Kreuzer, O. P., Etheridge, M. A., Guj, P., McMahon, M. E. and Holden, D. J., 2008. Linking mineral deposit models to quantitative risk analysis and decision-making in exploration. *Economic Geology*, **103**, 829-850pp.

Lambert, I., Jaireth, S., McKay, A. and Miezitis, Y., 2005. Why Australia has so much uranium. *Ausgeo News*, **80**, 7-10pp.

Laverov, N. P., Velitchkin, V. I. and Shumilin, M. V., 1992. Uranium deposits of the Commonwealth of Independant States: the main economic genetic types and their distribution (in Russian). *Geol Rudn Mestorozhd*, **2**, 3-18pp.

Matheson, I. and Hurtig, H. C., 2009. The Maureen U-Mo-F deposit. *Australian Institute of Geoscientists Bulletin*, **49**, 85-88pp.

McDermott, F., Harris, N. B. W. and Hawkesworth, C. J., 1996. Geochemical constraints on crustal anatexis: a case study from the Pan-African Damara granitoids of Namibia. *Contributions to Mineralogy and Petrology*, **123**, 406-423pp.

McKay, A. D. and Miezitis, Y., 2001. Australia's uranium resources, geology and development of deposits. 184p.

Minty, B. R. S., Franklin, R., Milligan, P. R., Richardson, L. M. and Wilford, J., 2009. Radiometric map of Australia (first edition) 1:5 000 000 scale. Geoscience Australia, Canberra.

Mysen, B. O., Cody, G. D. and Smith, A., 2004. Solubility mechanism of fluorine in peralkaline and meta-aluminous silicate glasses and in melts to magmatic temperatures. *Geochimica et Cosmochimica Acta*, **68**, 2745-2769pp.

Nex, P., Herd, D. and Kinnaird, J., 2002. Fluid extraction from quartz in sheeted leucogranites as a monitor to styles of uranium mineralization: an example from the Rössing area, Namibia. *Geochemistry: Exploration, Environment, Analysis*, **2**, 83-96pp.

Nex, P. A. M., Kinnaird, J. A. and Oliver, G. J. H., 2001. Petrology, geochemistry and uranium mineralisation of post-collisional magmatism around Goanikontes, southern Central Zone, Damaran Orogen, Namibia. *Journal of African Earth Sciences*, **33**, 481-502pp.

Nielsen, B. L. and Steenfelt, A., 1979. Intrusive events at Kvanefjeld in the Ilímaussaq igneous complex. *Bulletin of the Geological Society of Denmark*, **27**, 143-155pp.

Nykänen, V., Groves, D. I., Ojala, V. J., Eilu, P. and Gardoll, S. J., 2008. Reconnaissance-scale conceptual fuzzy-logic prospectivity modelling for iron oxide copper-gold deposits in the northern Ferroscandian Shield, Finland. *Australian Journal of Earth Sciences*, **55**, 25-38pp.

Peiffert, C., Cuney, M. and Nguyen-Trung, C., 1994. Uranium in granitic magmas: Part 1. Experimental determination of uranium solubility and fluid-melt partition coefficients in the uranium oxide-haplogranite-H_2O-Na_2CO_3 system at 720-770^oC, 2 kbar. *Geochimica et Cosmochimica Acta*, **58**, 2495-2507pp.

Peiffert, C., Nguyen-Trung, C. and Cuney, M., 1996. Uranium in granitic magmas: Part 2. Experimental determination of uranium solubility and fluid-melt partition coefficients in the uranium oxide-haplogranite-H_2O,-NaX (X = Cl, F) system at 770^oC, 2 kbar. *Geochimica et Cosmochimica Acta*, **60**, 1515-1529pp.

Plant, J. A., Simpson, P. R., Smith, B. and Windley, B. F., 1999. Uranium ore deposits: products of the radioactive earth. *Reviews in Mineralogy and Geochemistry*, **38**, 255-319pp.

Raymond, O. L., Liu, S. F., Whitaker, A. J., Stewart, A. J., Sweet, I. P., Needham, R. S., Retter, A. J., Phillips, D., Duggan, M. B., Champion, D. C., English, P. M., Connolly, D. P., Stewart, G., Hanna, A. L., Glanville, D. H., Fisher, C. L. and Kilgour, P., 2009. Surface geology of Australia 1:1,000,000 scale data package [digital dataset]. Canberra: The Commonwealth of Australia, Geoscience Australia.

Rogers, J. J. W. and Adams, J. A. S., 1969. Uranium. *Handbook of Geochemistry*. K. H. Wedepohl (ed). Berlin, Springer-Verlag. 11-17pp.

Rogers, J. J. W., Ragland, P. C., Nishimori, R. K., Greenberg, J. K. and Hauck, S. A., 1978. Varieties of granitic uranium deposits and favourable exploration areas in the eastern United States. *Economic Geology*, **73**, 1539-1555pp.

Rollinson, H., 1993. Using geochemical data: evaluation, presentation, interpretation. Harlow, Longman Group UK Ltd., 352p.

Sawka, W. N. and Chappell, B. W., 1986. The distribution of radioactive heat production in I- and S-type granites and residual source regions: implications for high heat flow areas in the Lachlan Fold Belt, Australia. *Australian Journal of Earth Sciences*, **33**, 107-118pp.

Sawka, W. N. and Chappell, B. W., 1987. Mafic xenoliths from I- and S-type granitoids: evidence for variations in deep crustal radioactive heat production. *Geophysical Research Letters*, **14**, 303-306pp.

Schofield, A., 2009. Uranium content of igneous rocks of Australia 1:5 000 000 maps: explanatory notes and discussion. *Geoscience Australia Record 2009/17*.

Schofield, A., 2010a. Potential for magmatic uranium systems in Australia. Map 1: intrusive-related. Geoscience Australia, Canberra. Available from www.ga.gov.au.

Schofield, A., 2010b. Potential for magmatic uranium systems in Australia. Map 2: volcanic-related. Geoscience Australia, Canberra. Available from www.ga.gov.au.

Skirrow, R. G., Jaireth, S., Huston, D. L., Bastrakov, E. N., Schofield, A., van der Wielen, S. E. and Barnicoat, A. C., 2009. Uranium mineral systems: Processes, exploration criteria and a new deposit framework. Geoscience Australia Record 2009/20.

Sørensen, H., 2001. Brief introduction to the geology of the Ilímaussaq alkaline complex, south Greenland, and its exploration history. *Geology of Greenland Survey Bulletin*, **190**, 7-23pp.

Sørensen, H. and Bailey, J. C., 2006. The origin and mode of emplacement of lujavrites in the Ilímaussaq alkaline complex, south Greenland. *Lithos*, **91**, 286-300pp.

Staatz, 1978. I and L uranium and thorium vein system, Bokan Mountain, Southeastern Alaska. *Economic Geology*, **73**, 512-523pp.

Sun, S. S. and McDonough, W. F., 1989. Chemical and isotope systematics of oceanic basalts: implications for mantle composition and processes. *Magmatism in the Ocean Basins*. A. D. Saunders and M. J. Norry (ed). Geological Society of London Special Paper 42. 313-345pp.

Thompson, T. B., 1988. Geology and uranium-thorium mineral deposits of the Bokan Mountain Granite Complex, southeastern Alaska. *Ore Geology Reviews*, **3**, 193-210pp.

Thompson, T. B., Pierson, J. R. and Lyttle, T., 1982. Petrology and petrogenesis of the Bokan Granite Complex, southeastern Alaska. *Geology*, **93**, 898-908pp.

Wall, V. J., 2006. Unconformity-related uranium systems: downunder and over the top. *Geological Society of Australia Abstracts*, **82**, 4p.

Walshe, J. L., Cooke, D. R. and Neumayr, P., 2005. Five questions for fun and profit: a mineral systems perspective on metallogenic epochs, province and magmatic hydrothermal Cu and Au deposits. *Mineral Deposit Research: Meeting the Global Challenge*, 477-480pp.

Watson, E. B. and Harrison, T. M., 1983. Zircon saturation revisited: temperature and composition effects in a variety of crustal magma types. *Earth and Planetary Science Letters*, **64**, 295-304pp.

Whalen, J. B., Currie, K. L. and Chappell, B. W., 1987. A-type granites: geochemical characteristics, discrimination and petrogenesis. *Contributions to Mineralogy and Petrology*, **95**, 407-419pp.

Zadeh, L. A., 1965. Fuzzy sets. *Information and control*, **8**, 338-353pp.

Appendix 1: Prospective units for intrusive-related U systems

SUPERSUITE	SUITE	UNIT	STRATNO	RATING
Almaden Supersuite		Hammonds Creek Granodiorite	8019	med-high
	Almaden Suite	Silver Pot Granodiorite	36171	med-high
	Kalunga Suite	Kalunga Granodiorite	27963	med-high
Babbage Supersuite	Moolawatana Suite	Box Bore Granite	23414	high
		Golden Pole Granite	23623	high
		Mount Neill Granite	12971	high
		Terrapinna Granite	17992	high
		Wattleowie Granite	29126	med-high
		Yerila Granite	20964	high
Ballandean Supersuite	Ballandean Suite	Ballandean Granite	41584	med-high
Bartle Frere Supersuite		Bartle Frere Granite	36181	med-high
Bathurst Supersuite	Bathurst Suite	Tarana Granite	17834	med-high
Bellenden Ker Supersuite	Bellenden Ker Suite	Bellenden Ker Granite	24177	med-high
Blue Mountains Supersuite		Morris Adamellite	12357	high
	Blue Mountains Suite	Blue Mountains Adamellite	1994	med-high
Boggy Plain Supersuite	Bogong Suite	Bogong Granite	2101	med-high
	Eugowra Suite	Eugowra Granite	27770	med-high
		Lords Granite	31715	med-high
	Grenfell Suite	Grenfell Granite	7795	med-high
	Gumble Suite	Gumble Granite	7872	med-high
	Mount Mittamatite Suite	Mount Mittamatite Granite	12938	med-high
	Nallawa Complex	Nallawa Complex	30909	med-high
	Thologolong Suite	Thologolong Granite	18061	med-high
	Yeoval Complex	Yeoval Complex	30531	med-high
	Yeoval Suite	Obley Granite	27053	high
		Yennora Granite	30523	med-high
Brodies Camp Supersuite		Knob Camp Granodiorite	36274	med-high
Bullenbalong Supersuite	Bullenbalong Suite	Happy Jacks Adamellite	25941	med-high
	Ingebyrah Suite	Biddi Granodiorite	25783	med-high

Bullenbalong Supersuite	Shannons Flat Suite	Shannons Flat Adamellite	16801	med-high
Callina Supersuite		Homeward Bound Granite	72356	med-high
Cape Melville Supersuite	Altanmoui Suite	Altanmoui Granite	27316	med-high
	Cape Melville Suite	Cape Melville Granite	30183	med-high
Cleland Supersuite		Strelley Monzogranite	69696	med-high
Cobargo Supersuite	Wangrah Suite	Danswell Creek Granodiorite	24240	high
		Wangrah Adamellite	24558	high
Cooktown Supersuite	Barrow Point Suite	Barrow Point Granite	69313	med-high
	Collingwood Suite	Collingwood Granite	30003	med-high
Cullen Supersuite	Allamber Springs Suite	Allamber Springs Granite - phase 1	72375	med-high
	Burnside Suite	Burnside Granite	26441	high
		Douglas Granite	30405	med-high
		Frances Creek Leucogranite	23601	med-high
	Fingerpost Suite	Minglo Granite - phase 1	72365	med-high
		Minglo Granite - phase 2	72366	med-high
	Margaret Suite	Mount Porter Granite	27050	med-high
		Prices Springs Granite	15576	med-high
	McMinns Bluff Suite	McMinns Bluff Granite	23781	med-high
	Saunders Suite	Saunders Granite	27056	med-high
	Shoobridge Suite	Tabletop Granite	27578	med-high
	Tennysons Suite	Fenton Granite	24275	med-high
		Tennysons Leucogranite	27058	med-high
Delegate Supersuite	Buckleys Lake Suite	Buckleys Lake Adamellite	2802	med-high
	Delegate Suite	Delegate Adamellite	25876	med-high
Durlacher Supersuite		Durlacher Supersuite	37648	med-high
Esmeralda Supersuite		Bimba Granite	27038	high
		Dregger Granite	28248	high
		Esmeralda Granite	6279	med-high
		Illewanna Granite	29208	high
		Macartneys Granite	27947	med-high
		Nonda Granite	24432	med-high
		Olsens Granite	23885	high

Fagan Supersuite		Jimbu Microgranite	32314	high
		Latram Granite	22174	high
		Packsaddle Microgranite	14735	high
Fiery Supersuite	Fiery Suite	Weberra Granite	19658	high
Forsayth Supersuite		Digger Creek Granite	5474	med-high
		Goldsmiths Granite	23624	med-high
		Mount Hogan Granite	24400	med-high
		Mywyn Granite	24416	med-high
Harcourt Supersuite	Barringo Suite	Barringo Granodiorite	1187	med-high
		Mount Disappointment Granodiorite	12638	med-high
	Harcourt Suite	Harcourt Granodiorite	8069	med-high
		Ingliston Granite	27436	med-high
	Tynong Suite	Tynong Granite	18759	med-high
		You Yangs Granite	21013	med-high
Hillgrove Supersuite	Gara Suite	Gara Monzogranite	41058	med-high
	Gostwyck Suite	Gostwyck Monzogranite	41061	med-high
	Hillgrove Suite	Hillgrove Adamellite	8349	med-high
	Murder Dog Suite	Murder Dog Monzogranite	69452	med-high
Hiltaba Supersuite	Hiltaba Suite	Balta Granite	1011	high
		Calca Granite	3312	high
		Charleston Granite	26473	med-high
		Hiltaba Suite	26613	med-high
Ingham Supersuite	Ingham Granite Complex	Ingham Granite Complex	36184	med-high
		Ingham Granite Complex - granodiorite to tonalite	69506	med-high
Kameruka Supersuite	Jingo Creek Suite	Jingo Creek Adamellite	22036	high
Kangaroo Creek Supersuite		Copper Bush Granite	36284	med-high
Kintore Supersuite		Kintore Supersuite	9629	med-high
	Ebagoola Suite	Ebagoola Granite	23570	med-high
Koetong Supersuite	Koetong Suite	Koetong Granite	9701	med-high
		Weethalle Granite	25610	med-high
		Yalgogrin Granite	36151	med-high
	Ungarie Suite	Wargin Granite	29580	med-high

Lags Supersuite		Bustlem Microgranite	3198	med-high
		Saint Helena Monzogranite	22803	med-high
	Lags Suite	Yokas Microgranite	24143	med-high
	Maneater Suite	Maneater Granodiorite	23760	med-high
Leichhardt Supersuite		Emysland Granodiorite	36212	med-high
		Mingoom Granite	11912	med-high
Mole Supersuite	Dumboy-Gragin Suite	Dumboy-Gragin Granite	5798	med-high
	Elsmore Suite	Elsmore Granite	6114	med-high
	Gilgai Suite	Gilgai Granite	7218	med-high
	Mole Suite	Mole Granite	12035	med-high
Moonbi Supersuite	Oban Suite	Kingsgate Leucogranite	37189	med-high
		Red Range Microleucogranite	38271	med-high
Moorarie Supersuite		Dumbie Granodiorite	36887	med-high
O'Briens Creek Supersuite		Askins Microgranite	36247	high
		Charlies Knob granite	36590	med-high
		Desert Creek granite	36594	med-high
		Flynns Creek Granite	36106	med-high
		Fulford Creek granite	36587	med-high
		Neds Gully Granite	36248	med-high
		Pat and Peter Creek granite	37928	high
		Square Rock granite	36585	med-high
	Burlington Suite	Burlington Granite	37808	high
	Cherry Tree Suite	Atlanta Granite	27697	med-high
		Jumna Granite	22043	med-high
		Lass O'Gowrie Granite	22172	med-high
	Go Sam Suite	Go Sam Granite	7464	high
		Mount Gibson Microgranite	12745	high
		Percy Granophyre	15063	high
		Pinnacles Granite	15267	high
		Top Nettle Microgranite	18423	high
	McCord Suite	McCord Granite	11533	med-high
	Nettle Suite	Billings Granite	23386	med-high

O'Briens Creek Supersuite	Nettle Suite	Black Prince Granite	36162	med-high
		Cigarette Granite	23489	med-high
		Emuford Granite	23581	med-high
	O'Briens Creek Suite	Elizabeth Creek Granite	28530	med-high
		Lancewood Rhyolite	36484	med-high
	Ravenshoe Suite	Ravenshoe Granite	15867	high
O'Callaghans Supersuite	Mount Crofton Suite	Mount Crofton Granite	12602	med-high
Ootann Supersuite		Ixe Microgranodiorite	8815	med-high
		Kitchener Granite	29311	med-high
		Ootann Supersuite	14620	med-high
		Princess Hills Granite	23920	med-high
		Sandy Tate Granite	36228	med-high
		Sheba Granite	29332	med-high
		Whistler Granite	36221	med-high
	Gurrumba Ring Complex	Gurrumba Ring Complex	7931	med-high
	Ootann Suite	Bamford Granite	21188	med-high
		Halpin Granite	21938	med-high
		Indicator Granite	21997	med-high
		Pandora Granite	14815	med-high
		Petford Granite	27878	med-high
		Sunnymount Granodiorite	30422	med-high
	Saucebottle Suite	Saucebottle Granite	29331	med-high
	Watsonville Suite	Watsonville Granite	19601	med-high
Oweenee Supersuite	Coane Range Granite Complex	Coane Range Granite Complex	4212	med-high
Paperbark Supersuite		Kongorow Granite	9760	med-high
		Lennard Granite	10340	med-high
		Louisa Monzogranite	30670	med-high
		Mondooma Granite	12089	med-high
		Nellie Tonalite	13975	high
		Paperbark Supersuite	31788	high
		Scrutons Monzogranite	29212	med-high
		Secure Bay Monzogranite	16723	med-high

Paperbark Supersuite		sheared granite 74499	74499	med-high
Pieter Botte Supersuite	Nulbullulul Suite	Bunk Creek Granite	29999	med-high
Pitjantjatjara Supersuite		Umbeara granites	42440	med-high
	Kulpitjata Suite	Kulpitjata Suite	42439	med-high
	Mantarurr Granite Suite	Mantarurr Granite Suite	33648	med-high
	Pottoyu Granite Suite	Pottoyu Granite Suite	33649	med-high
	Umutju Granite Suite	Umutju Granite Suite	33650	med-high
Round Mountain Supersuite	Round Mountain Suite	Round Mountain Leucoadamellite	16389	med-high
Sally Downs Supersuite	Shepherds Bore Plutonic Complex	Shepherds Bore Plutonic Complex	30591	med-high
Sisters Supersuite		Mungarinya Monzogranite	35351	med-high
		Petermarer Monzogranite	35234	med-high
		Powdar Monzogranite	33203	med-high
	Yule Granitoid Complex	Pilbara Creek Monzogranite	35352	high
Split Rock Supersuite		Numbana Monzogranite	38012	med-high
Stanthorpe Supersuite	Bolivia Range Suite	Bolivia Range Leucomonzogranite	38267	med-high
		Dandahra Creek Leucogranite	5174	high
	Bungulla Suite	Bookookoorara Monzogranite	73824	med-high
	Stanthorpe Suite	Mackenzie Monzogranite	38266	med-high
		Ruby Creek Granite	16417	med-high
		Stanthorpe Granite 1	73853	med-high
		Stanthorpe Granite 2	73855	med-high
		Stanthorpe Granite 3	73856	med-high
		Stanthorpe Granite 5	73858	med-high
Tennant Creek Supersuite		Cabbage Gum Granite	3256	med-high
		Channingum Granite	3910	med-high
		Hill of Leaders Granite	24310	med-high
		Mumbilla Granodiorite	22471	med-high
		Tennant Creek Granite	17951	med-high
The Granites Supersuite		Lewis Granite	10363	med-high
		Winnecke Granophyre	20256	high
Tulendeena Supersuite	Russells Road Suite	Tombstone Creek Granite	18315	med-high
Uralla Supersuite	Mount Duval Suite	The Basin Monzogranite	67910	med-high

Uralla Supersuite	Mount Duval Suite	Tingha Monzogranite	38354	med-high
	Webbs Consols Suite	Webbs Consols Leucogranite	19657	med-high
Weymouth Supersuite		Weymouth Granite	19856	med-high
White Springs Supersuite		Robin Hood Granodiorite	16185	med-high
		White Springs Supersuite	36107	med-high
Whypalla Supersuite	Curraghmore Suite	Nangee Granite	23861	med-high
Williams Supersuite		Mount Angelay Granite	24390	high
		Mount Dore Granite	24396	high
		Naraku Granite	13847	med-high
		Saxby Granite	26324	high
		Williams Granite	20083	med-high
	Squirrel Hills Suite	Mount Cobalt Granite	24393	high
		Squirrel Hills Granite	24501	high
		Wimberu Granite	27935	high
		Yellow Waterhole Granite	24599	high
Willyama Supersuite	Basso Suite	Basso Suite	35879	high
Woodstock Supersuite	Mundic Igneous Complex	Mundic Igneous Complex	13438	med-high
	Woodstock Suite	Magnetic Island Granite	11011	med-high
		Mount Storth Granite	23833	med-high
Younger Lincoln Supersuite		Carappee Granite	3572	high
	Moody Suite	Wertigo Granite	24094	med-high
	Alarinjela Suite	Marshall Granite	11378	med-high
	Allia Suite	Allia Creek Granite	303	med-high
		Murra-Kamangee Granodiorite	26787	med-high
	Angatja Suite	Angatja Suite	42420	med-high
	Ararat Suite	Ararat Granodiorite	533	med-high
		Stawell Granite	17308	med-high
	Ardlethan Suite	Ardlethan Granite	554	med-high
	Argylla Suite	Bowlers Hole Granite	24196	high
	Atneequa Granitic Complex	Atneequa Granitic Complex	23344	med-high
	Bangadilly Suite	Bangadilly Granodiorite	21192	med-high
	Barrow Creek Granite Complex	Barrow Creek Granite Complex	27283	med-high

	Beckworth Suite	Ercildoun Granite	6227	med-high
		Mount Bute Granite	12560	med-high
	Bedarra Granite Complex	Bedarra Granite Complex	36415	med-high
	Bimbowrie Suite	Bimbowrie Suite	69582	med-high
	Bindogandri Suite	Bindogandri Granite	28368	med-high
	Blanket Flat Suite	Blanket Flat Granite	1926	med-high
	Bogalong Suite	Bogalong Suite	31620	med-high
	Boobyalla Suite	Ansons Bay Adamellite	26347	med-high
		Kent Bay Granite	9445	med-high
		Key Bay Granite	69575	high
		Maria Island Granite	11298	med-high
	Bradshaw Suite	Drimmie Head Granite	21695	med-high
	Burstall Suite	Burstall Granite	25823	med-high
		Mount Erle Igneous Complex	24398	high
		Myubee Igneous Complex	24415	med-high
		Overlander Granite	24446	high
		Revenue Granite	24471	high
		Saint Mungo Granite	24485	med-high
	Caragabal Suite	Caragabal Granite	3566	med-high
	Cobaw Suite	Baynton Granodiorite	1286	med-high
		Pyalong Granite	15694	med-high
	Collingullie Suite	Collingullie Granite	23496	med-high
	Cowie Suite	Cowie Granite	27951	high
	David Suite	Eva Valley Granite	6401	med-high
		Grace Creek Granite - phase 2	72369	high
		Grace Creek Granite - phase 3	72370	high
		Grace Creek Granite - phase 4	72371	high
		Jim Jim Granite	8956	med-high
		Malone Creek Granite - phase 1	72372	high
		Malone Creek Granite - phase 2	72373	high
		Malone Creek Granite - phase 3	72374	high
		Nabarlek Granite	13671	med-high

	David Suite	Tin Camp Granite	18189	high
		Elkedra Granite	25892	med-high
	Donington Suite	Donington Suite	5603	med-high
	Dutton Suite	Dutton Suite	5878	med-high
	Ellenden Suite	Ellenden Granite	25893	med-high
	Ellery Suite	Ellery Granite	6095	med-high
	Erimeran Suite	Erimeran Granite	25898	med-high
	Free Damper Suite	Free Damper Adamellite	32241	med-high
	Freycinet Suite	Coles Bay Adamellite	33473	med-high
		Freycinet Granite	6910	high
		Schouten Island Granite	26889	high
		The Hazards Granite	26937	high
	Gabo Suite	Gabo Island Granite	6946	high
		Howe Range Granite	26622	high
		Nagha Granite	13682	high
		Naghi Adamellite	22500	high
		Watergums Adamellite	23153	high
	Giddy Suite	Bukudal Granite	21356	med-high
		Dhalinybuy Granite	21653	high
		Garthalala Granite	21834	med-high
		Giddy Granite	27414	high
	Glen Esk Suite	Glen Esk Adamellite	26576	med-high
	Gobondery Suite	Gobondery Granite	7469	med-high
	Gregory Range Suite	Gregory Range Suite	73504	high
	Grimwade Suite	Grimwade Suite - group 1	72648	med-high
		Grimwade Suite - group 3	72650	med-high
		Grimwade Suite - group 5	72652	med-high
	Gundibindyal Suite	Gundibindyal Granite	29581	med-high
	Harverson Suite	Anmatjira Granite	26346	high
	Henbury Suite	Henbury Granite	40854	med-high
	Hogan Island Suite	Hogan Island Granite	26616	med-high
	Housetop Suite	Dolcoath Granite	5570	med-high

	Housetop Suite	Housetop Granite	8532	med-high
	Hull Granite Suite	Hull Granite Suite	36768	high
	Illili Suite	Illili Suite	41845	med-high
	Interview Suite	Interview Granite	8743	med-high
	Jervois Suite	Dneiper Granite	5548	high
	Jindera Suite	Jindera Granite	8980	med-high
	Jingera Rock Syenite Complex	Jingera Rock Syenite Complex	8987	med-high
	Jinka Suite	Jinka Granite	26643	high
		Mount Ida Granite	12816	med-high
		Mount Swan Granite	13125	high
	Kellys Creek Suite	Kellys Creek Leucomonzogranite	73842	med-high
	Kyeamba Suite	Burrandana Granite	3126	med-high
		Kyeamba Suite	31597	med-high
	Lyndbrook Complex	Lyndbrook Complex	39611	med-high
	Madderns Yard Metamorphic Complex	Talipata Granite	37706	high
	Mannus Creek Suite	Bogandyera Granite	2084	med-high
	Medicine Creek Complex	Medicine Creek Complex	30104	med-high
	Meredith Suite	Wombat Flat Granite	20401	high
	Monga Suite	Monga Granite	12098	med-high
	Mordor Igneous Complex	Mordor Igneous Complex	25731	med-high
	Mount Bridgman Igneous Complex	Mount Bridgman Igneous Complex	70141	med-high
	Mount Leinster Igneous Complex	Mount Leinster Igneous Complex	26764	high
	Mount Misery Suite	Mount Misery Granite	12933	med-high
	Mount Painter Complex	Pepegoona Porphyry	15047	high
	Mount Webb Suite	Mount Webb Granite	13203	med-high
	Mumbulla Suite	Doctor George Granite	23549	high
		Mumbulla Granite	23848	med-high
	Musselroe Suite	Modder River Granite	12003	med-high
	Nanambu Complex	Nanambu Complex	27856	med-high
	Napperby Suite	Possum Creek Charnockite	26321	med-high
		Uldirra Porphyry	24546	high
		Wangala Granite	24556	high

	Narraburra Suite	Narraburra Granite	13890	high
	Nicholson Granite Complex	Nicholson Granite Complex - phase a	72378	high
		Nicholson Granite Complex - phase b	72379	med-high
	Nimbuwah Complex	Nimbuwah Complex - granite	72396	med-high
	Nymagee Igneous Complex	Nymagee Igneous Complex	26087	med-high
	Pieman Suite	Pieman Granite	15177	med-high
	Poimena Suite	Poimena Adamellite	15358	med-high
	Promontory Suite	Lilly Pilly Granite	25166	med-high
		Rodondo Island Granite	28970	med-high
		Vereker Granite	26974	med-high
		Wilsons Promontory Granite	20179	med-high
	Royal George Suite	Gipps Creek Granite	40851	med-high
	Rum Jungle Complex	Rum Jungle Complex	16439	med-high
	Saint Francis Suite	Saint Francis Suite	34338	high
	Southwark Suite	Southwark Suite	40018	high
		Wabudali Granite	23115	med-high
		Yaloolgarrie Granite	31339	med-high
		Yarunganyi Granite	23298	med-high
		Yunkanjini Granite	72410	high
	Spilsby Suite	Spilsby Suite	17164	med-high
	St Peter Suite	St Peter Suite	24502	med-high
	Strathbogie Suite	Strathbogie Granite	17408	med-high
	Sybella Suite	Annable Granite	30693	med-high
		Briar Granite	30705	high
		Easter Egg Granite	30694	high
		Gidya Granite	30695	high
		Hay Mill Granite	30697	high
		Kahko Granodiorite	30699	med-high
		Keithys Granite	30700	high
		Kitty Plain microgranite	28054	high
		Queen Elizabeth Granite	30701	high
		Steeles Granite	30702	high

	Sybella Suite	Sybella Granite	17589	med-high
		Widgewarra Granite	30703	high
		Wonomo Granite	23243	high
	Ulandra Suite	Ulandra Granite	28302	med-high
	Wagait Suite	Koolendong Granite	9772	med-high
		Peppimenarti Granite	24454	med-high
	Waluwiya Suite	Russell Charnockite	41851	med-high
	Warburton Suite	Warburton Granodiorite	25597	med-high
	Whipstick Suite	Whipstick Adamellite	24098	high
	Wonga Suite	Birds Well Granite	24183	med-high
		Wonga Granite	27938	high
	Woodgreen Granite Complex	Woodgreen Granite Complex	28280	med-high
	Woolton Granite Complex	Woolton Granite Complex	32150	med-high
	Wuluma Suite	Gum Tree Granite	7869	med-high
	Wyangala Suite	Bigga Granite	1608	med-high
	Wybalenna Suite	Cape Sir John Granodiorite	23466	med-high
	Yabba Suite	Yabba Granite	20736	med-high
	Yammatree Suite	Yammatree Granite	20793	med-high
	Yeldham Suite	Yeldham Granite	20928	med-high
		Asylum Granite	33796	med-high
		Bayfield Granite	1283	med-high
		Beauvallet Granodiorite	32493	med-high
		Bewilder Granite	36437	med-high
		Blackmans Creek Granite, Spring Road Granite	42004	med-high
		Boginderra Granite	23400	med-high
		Boolahbone Granite	24748	high
		Boolgal Granophyre	35036	med-high
		Bow River Granite	2394	med-high
		Broomfield Granite	2647	med-high
		Broula Granite	29521	med-high
		Bullabulling Monzogranite	2884	med-high
		Butcher Bird Monzogranite	34924	med-high

		Canoe Creek Granite	33429	med-high
		Cape Willoughby Granite	34794	med-high
		Castletower Granite	24830	med-high
		Cleethorpes Granodiorite	33152	med-high
		Coan Granite	25849	med-high
		Crockers Well Granite	35402	high
		Crows Nest Granite	4958	med-high
		Dingo Mountain Granodiorite	36428	med-high
		Dove Granite	29241	med-high
		Elliott Bay Granite	69573	med-high
		Esther Granite	70576	med-high
		felsic intrusives 42022	42022	med-high
		felsic intrusives 42189	42189	med-high
		Ganantagi Granite	6987	med-high
		Gidley Granophyre	7187	med-high
		Gilgunnia Granite	7222	med-high
		Gin Creek Granite	7245	med-high
		Glenleigh Granite	32148	med-high
		Goonoonglah Monzodiorite, Yewangara Granite, Sentry Box Granite	42003	med-high
		granite - Olary Domain 74182	74182	high
		granite, pegmatite 74405	74405	med-high
		granitoids - Syn-Kimban Orogeny 73072	73072	med-high
		Grevillea Granite	39067	med-high
		Heemskirk (red) Granite	8243	high
		Heemskirk (white) Granite	26609	med-high
		high-HFSE granite 74295	74295	med-high
		Hivesville Granite	33425	med-high
		Hogback Granite	25061	med-high
		House and Kitchen Granite	21979	med-high
		Illoura Granodiorite	37748	med-high
		Kaidwalla Granite	72697	high

		Koonoonyeri Granite	72419	high
		Lake Dundas Monzogranite	67870	med-high
		Lewin Springs Syenite	23724	med-high
		Licking Gully Granite	35614	med-high
		Lockhart Granite	37573	med-high
		Logue Brook Granite	23735	med-high
		low-Ca granite 74297	74297	med-high
		Milmiland Granite	29555	med-high
		Morang Granodiorite	12311	med-high
		Mount Allen Granite	12454	med-high
		Mount Foster Monzonite	32376	high
		Mount Norgate Granite	37764	med-high
		Mount Taylor Granite	13129	med-high
		Nerrely Leucogranite	73468	med-high
		Palmer Granite	14804	med-high
		Poison Creek Granite	22670	med-high
		Purkin Granite	25420	med-high
		Pyramid Hill Granite	15707	med-high
		Redhackle Granite	70535	med-high
		Roscow Granite	30890	med-high
		Samarkand Pegmatite	26131	med-high
		Schneiders Granite	33684	med-high
		The Brothers Granitoids	69453	med-high
		Toondahra Granite	18404	med-high
		Trungley Hall Granite	24046	med-high
		Ularring Monzogranite	34584	med-high
		Urambie Granodiorite	18975	med-high
		Urapunga Granite	30318	med-high
		Victoria Valley Granite	19112	med-high
		Wakooka Granite	30189	med-high
		Warimbi Schist	26331	med-high
		White Crystal Granite	23187	med-high

		Woondum Granite	20601	med-high
		Xanten Granite	24128	med-high
		Yanakie Granite	25661	med-high
		Yarra Granite	20859	med-high
		Yellow Mountain Granite	20939	med-high

Notes:
- ‘STRATNO’ denotes the Australian stratigraphic unit number assigned to the unit listed in the ‘UNIT’ column. For more information see http://dbforms.ga.gov.au/www/geodx.strat_units.int
- Units listed here do not include units in New South Wales, Victoria or Tasmania, since those states currently do not permit U exploration and/or mining. Some units may cross borders into these states, but are included here for completeness
- ‘Medium-high’ denotes prospectivity in the range 0.6-0.8. ‘High’ denotes prospectivity >0.8

Appendix 2: Prospective units for volcanic-related U systems

SUPERGROUP	GROUP	UNIT	STRATNO	RATING
Bentley Supergroup	Tollu Group	Smoke Hill Volcanics	17012	med-high
Boggy Plain Supersuite	Boraig Group	Boraig Group	24753	med-high
	Hyandra Creek Group	Hyandra Creek Group	8619	med-high
Cobar Supergroup		Tarran Volcanics	24013	med-high
	Kopyje Group	Babinda Volcanics	25702	med-high
		Florida Volcanics	6774	med-high
		Majuba Volcanics	27473	med-high
		Mineral Hill Volcanics	11894	high
	Mount Hope Group	Mount Hope Group	25281	med-high
	Rast Group	Gurragong Volcanics	40131	med-high
	Rast Group	Ural Volcanics	18968	med-high
Esmeralda Supersuite	Croydon Volcanic Group	B Creek Rhyolite	24167	high
		Carron Rhyolite	26297	med-high
		Democrat Rhyolite Member	24242	high
		Idalia Rhyolite	24314	high
		Parrot Camp Rhyolite	24451	high
		Wonnemarra Rhyolite	24583	high
Fiery Supersuite		Fiery Creek Volcanics	6639	med-high
		Peters Creek Volcanics - units 2 to 7	69039	med-high
Mount Read Volcanics	Tyndall Group	Tyndall Group	18756	med-high
Ootann Supersuite	Ootann Suite	Cottell Rhyolite	21565	med-high
Oweenee Supersuite		Oweenee Rhyolite	24447	med-high
		Paluma Rhyolite	23891	med-high
Paperbark Supersuite		Bickleys Porphyry	1575	med-high
Younger Lincoln Supersuite		McGregor Volcanics	23777	med-high
	Black Range Group	Pilleuil Andesite, Waynes Knob Rhyolite, Sharpeningstone Conglomerate	41967	med-high
	Boyd Volcanic Complex	Boyd Volcanic Complex	27117	med-high
	Bredbo Group	Colinton Volcanics	4334	med-high

	Bredbo Group	Williamsdale Dacite Member	20085	med-high
	Bulgonunna Volcanic Group	Bulgonunna Volcanic Group	2867	med-high
	Campbells Group	Kangaloolah Volcanics	9206	med-high
	Carrara Range Group	Carrara Range Group	3679	med-high
	Cootamundra Group	Cowcumbala Rhyolite	27135	med-high
	Cudal Group	Canowindra Volcanics, Nargong Volcanics	42000	med-high
	Cumberland Range Volcanic Group	Scrubby Creek Rhyolite	23959	high
	Currangandi Group	Taggarts Mountain Ignimbrite Member	17648	med-high
	Dartella Volcanic Group	Dartella Volcanic Group	23535	med-high
	Donydji Group	Fagan Volcanics	24971	med-high
	Douro Group	Deakin Volcanics	25874	med-high
		Goobarragandra Volcanics	25929	med-high
		Hawkins Volcanics	8184	med-high
		Laidlaw Volcanics	10024	med-high
		Mount Ainslie Volcanics	12438	med-high
		Walker Volcanics	19240	med-high
	Edith River Group	Plum Tree Creek Volcanics	15334	med-high
	El Sherana Group	Pul Pul Rhyolite	15650	high
	Enano Group	Thorkidaan Volcanics, Mitta Mitta Rhyolite	37697	med-high
	Featherbed Volcanic Group	Beapeo Rhyolite	27976	med-high
		Boonmoo Volcanic Subgroup	27966	med-high
		Djungan Volcanic Subgroup	21673	high
		Jamtin Rhyolite	22016	high
		Nightflower Dacite	23874	med-high
		Redcap Dacite	22738	med-high
		Tennyson Volcanic Subgroup	27967	med-high
		Timber Top Volcanic Subgroup	23003	high
		Wakara Volcanic Subgroup	23117	med-high
		Yongala Volcanic Subgroup	27971	med-high
	Finniss River Group	Berinka Volcanics	1503	med-high
	Gawler Range Volcanics	Bittali Rhyolite	23390	med-high
		Bunburn Dacite	25818	med-high

	Gawler Range Volcanics	Carnding Rhyodacite	23472	med-high
		Ealbara Rhyolite	23568	med-high
		Eucarro Rhyolite	36782	med-high
		Gawler Range Volcanics	7059	high
		Lake Gairdner Rhyolite	25985	med-high
		Waganny Dacite	24068	med-high
		Wheepool Rhyolite	19865	med-high
		Yantea Rhyodacite	26241	med-high
		Yardea Dacite	20845	med-high
	Gnalta Group	Gnalta Group	7460	med-high
	Hatches Creek Group	Wauchope Subgroup, Lower	39130	med-high
	Hawkins Volcanic Suite	Paddys River Volcanics	26093	med-high
	Janet Ranges Volcanic Group	Janet Ranges Volcanics	8869	high
	Koolmoon Volcanic Group	Glen Gordon Volcanics	7340	med-high
		Slaughter Yard Creek Volcanics	16991	med-high
		Walsh Bluff Volcanics	19332	med-high
	Laidlaw Volcanic Suite	Uriarra Volcanics	18992	med-high
	Mount Fairy Group	Mount Fairy Group	26052	med-high
	Mount Little Volcanic Group	Linley Rhyolite	23729	med-high
	Mumbil Group	Bells Creek Volcanics	24709	med-high
	Nandewar Volcanic Complex	felsic to intermediate volcanics and high level intrusives 68002	68002	high
	Newcastle Range Volcanic Group	Bousey Rhyolite	23413	med-high
		Brodies Gap Rhyolite	2609	med-high
		Kitchen Creek Rhyolite	28116	med-high
		Routh Dacite	16392	med-high
	Nicholson Suite	Cliffdale Volcanics	4151	med-high
	Ooradidgee Group	Bernborough Formation	1514	med-high
		Epenarra Volcanics	27287	med-high
		Mia Mia Volcanics	26313	med-high
		Treasure Volcanics	24535	med-high
		Warrego Volcanics	19520	high

	Rocky Ponds Group	Dulladerry Volcanics	29509	high
		Warrumba Volcanics	32474	med-high
	Scardons Volcanic Group	Dickson Creek Rhyolite	36281	high
		Red River Rhyolite	36278	med-high
	Sophie Downs Suite	Ding Dong Downs Volcanics - felsic volcanics	74376	med-high
	Spencer Creek Group	Yanungbi Volcanics	23289	med-high
	St Peter Suite	Nuyts Volcanics	24435	med-high
	Sybella Suite	Carters Bore Rhyolite	3701	med-high
	Tawallah Group	Hobblechain Rhyolite	8388	med-high
	Tewinga Group	Argylla Formation	585	high
		Leichhardt Volcanics	28675	med-high
		Tewinga Group	25525	med-high
	Tjauwata Group	Puntitjata Rhyolite	33811	med-high
	Trundle Group	Trundle Group	29079	med-high
	Wandsworth Volcanic Group	Annalee Pyroclastics	24660	med-high
		Drake Volcanics	28513	med-high
		Emmaville Volcanics	6143	med-high
		Gibraltar Ignimbrite	7167	med-high
		Wallangarra Volcanics	19265	med-high
		Wandsworth Volcanic Group	29113	med-high
	Ware Group	Mount Winnecke Formation - felsic volcanic facies	72667	med-high
		Blowering Formation	27671	med-high
		Cape Grenville Volcanics	27126	med-high
		Comerong Volcanics	25853	med-high
		felsic extrusives 69834	69834	med-high
		felsic to intermediate volcanics and high level intrusives 42180	42180	high
		felsic volcanic rocks 74291	74291	med-high
		felsic volcanics and high level intrusives 39449	39449	med-high
		felsic volcanics and high level intrusives 42173	42173	med-high
		felsic volcanics and high level intrusives 42193	42193	high
		Frampton Volcanics	6881	med-high

		Ginninderra Porphyry	7262	med-high
		Greybank Volcanics	23638	high
		Ina Volcanics	24315	high
		Junalki Formation	22045	med-high
		Koongie Park Formation	9793	med-high
		Nanyeta Volcanics	26798	med-high
		Nychum Volcanics	27864	med-high
		Paddock Creek Formation	23889	med-high
		Paterson Volcanics	14945	med-high
		Peak Range Volcanics	14970	high
		Pratt Volcanics	22693	med-high
		Reamba Volcanics	36103	med-high
		Scrutton Volcanics	16698	med-high
		Wallaman Falls Volcanics	36340	med-high
		Walleroobie Volcanics	27603	med-high
		Whitewater Volcanics	19928	med-high

Notes:

- 'STRATNO' denotes the Australian stratigraphic unit number assigned to the unit listed in the 'UNIT' column. For more information see http://dbforms.ga.gov.au/www/geodx.strat_units.int
- Units listed here do not include units in New South Wales, Victoria or Tasmania, since those states currently do not permit U exploration and/or mining. Some units may cross borders into these states, but are included here for completeness
- 'Medium-high' denotes prospectivity in the range 0.6-0.8. 'High' denotes prospectivity >0.8